PROBABILISTIC CONFORMAL PREDICTION WITH APPROXIMATE CONDITIONAL VALIDITY

Anonymous authors
Paper under double-blind review

ABSTRACT

We develop a new method for generating prediction sets that combines the flexibility of conformal methods with an estimate of the conditional distribution $\mathrm{P}_{Y|X}$. Existing methods, such as conformalized quantile regression and probabilistic conformal prediction, usually provide only a marginal coverage guarantee. In contrast, our approach extends these frameworks to achieve approximately conditional coverage, which is crucial for many practical applications. Our prediction sets adapt to the behavior of the predictive distribution, making them effective even under high heteroscedasticity. While exact conditional guarantees are infeasible without assumptions on the underlying data distribution, we derive non-asymptotic bounds that depend on the total variation distance of the conditional distribution and its estimate. Using extensive simulations, we show that our method consistently outperforms existing approaches in terms of conditional coverage, leading to more reliable statistical inference in a variety of applications.

1 INTRODUCTION

Conformal prediction methods are often used to generate prediction sets because they provide finite sample validity under minimal assumptions (Vovk et al., 2005; Shafer & Vovk, 2008). However, their performance can degrade in the presence of heteroscedasticity (Dewolf et al., 2023). The split-conformal approach uses a calibration dataset of size n, denoted as $\{(X_k, Y_k)\}_{k\in[n]}$ with $X_k \in \mathbb{R}^d$ and $Y_k \in \mathcal{Y}$ to construct prediction sets $\mathcal{C}_\alpha(x)$ for a chosen confidence level $\alpha \in (0,1)$. For each $x \in \mathbb{R}^d$, the prediction set based on a conformity score function $V\colon \mathbb{R}^d \times \mathcal{Y} \to \mathbb{R}$, is given by

$$\mathcal{C}_\alpha(x) = \left\{ y \in \mathcal{Y}\colon V(x,y) \leq Q_{1-\alpha}\left(\frac{1}{n+1} \sum\nolimits_{k=1}^{n} \delta_{V(X_k,Y_k)} + \frac{1}{n+1}\delta_\infty \right) \right\}, \tag{1}$$

where δ_x is the Dirac mass and $Q_{1-\alpha}(\mu)$ is the $(1-\alpha)$-quantile of the probability μ. If the calibration data $\{(X_k, Y_k)\}_{k\in[n]}$ is drawn i.i.d. from a population distribution $\mathrm{P}_{X,Y}$, then for any new data point $(X_{n+1}, Y_{n+1}) \sim \mathrm{P}_{X,Y}$ sampled independently of the calibration data, the conformal theory ensures the *marginal validity* of $\mathcal{C}_\alpha(X_{n+1})$, meaning that $\mathbb{P}\left(Y_{n+1} \in \mathcal{C}_\alpha(X_{n+1})\right) \geq 1-\alpha$. This marginal guarantee can hide significant discrepancies in the coverage of different regions of the input space $\mathbb{R}^d$; see e.g. Izbicki et al. (2022); Hore & Barber (2024). Conditional validity is a more desirable guarantee than marginal validity: for any $x \in \mathbb{R}^d$, the set $\mathcal{C}_\alpha(x)$ is *conditionally valid* if

$$\mathbb{P}\left(Y_{n+1} \in \mathcal{C}_\alpha(X_{n+1}) \mid X_{n+1} = x\right) \geq 1-\alpha. \tag{2}$$

However, this property cannot be achieved without further assumptions about the data distribution; see Vovk (2012); Lei & Wasserman (2014). For practical purposes, it is enough to construct sets $\mathcal{C}_\alpha$ which approximate (2), and ideally achieve it asymptotically under suitable conditions in the limit of large sample size n.

RELATED WORK

Conformal prediction with conditional guarantees. A great deal of research has been devoted to this problem, starting with the case where $\mathcal{Y} = \mathbb{R}$. For example, Romano et al. (2019) and Kivaranovic et al. (2020) proposed methods based on estimate of the lower and upper conditional quantile function $\hat{q}_{\alpha/2}$ and $\hat{q}_{1-\alpha/2}$, to define a quantile-based conformity score:

$V(x, y) = \max\left\{\hat{q}_{\alpha/2}(x) - y, y - \hat{q}_{1-\alpha/2}(x)\right\}$ which is then conformalized. Improvements of this conformity score are investigated in Kivaranovic et al. (2020). Sesia & Candès (2020) have shown that the constructed interval converges to the narrowest possible interval that achieve conditional coverage under mild assumptions. We stress that these methods are specific to the case $\mathcal{Y} = \mathbb{R}$; in addition, when the conditional distribution $\mathrm{P}_{Y|X}$ is multimodal, restricting prediction to intervals is suboptimal; see Wang et al. (2023) for a discussion and examples. It has been suggested in Guan (2023); Alaa et al. (2023); Hore & Barber (2024) to partition $\mathbb{R}^d$ and learn a specific quantile for each regions. Splitting the space $\mathbb{R}^d$ into multiple regions typically leads to an increase in the length of the prediction set; see Romano et al. (2020a); Melki et al. (2023) for comments.

Conformal prediction based on estimates of conditional distribution. A number of studies have focused on the construction of prediction sets using an estimator of the conditional distribution $\mathrm{P}_{Y|X}$. Again, in the case where $\mathcal{Y} = \mathbb{R}$, Cai et al. (2014); Lei & Wasserman (2014) have constructed prediction intervals based on an estimator of the conditional density and have established the asymptotic validity under appropriate conditions. Han et al. (2022) use kernel density estimation to construct asymmetric prediction bands. However, this method cannot handle bimodality as it generates a single interval. On the other hand, Sesia & Romano (2021) partition the domain of Y into bins to create a histogram approximation of $\mathrm{P}_{Y|X}$. The authors showed that their method satisfies the marginal validity while achieving the asymptotic conditional coverage; see also Lei et al. (2018). Asymptotic conditional coverage is also obtained using quantile regression-based methods (Sesia & Candès, 2020; Cauchois et al., 2020), or using cumulative distribution function estimators (Izbicki et al., 2020; Chernozhukov et al., 2021). Conditionally valid prediction sets have been shown to improve the robustness to perturbations (Gendler et al., 2021). Guha et al. (2024) proposed a novel approach that converts regression tasks into classification problems by binning the output space. Leveraging this discretization, they approximate the conditional density to construct prediction sets that correspond to HPD regions. A limitation lies in the discretization process, as the number of labels required for complex scenarios can become computationally prohibitive. The method developed by Kiyani et al. (2024) enhances adaptive coverage by learning a family of weights that automatically adjust the quantile of the conformity score in function of the covariate x. An explicit control of the mean squared error between the conditional coverage and the confidence level $1 - \alpha$ is also provided.

Conformal prediction for multi-output regression. Very few studies have addressed the scenario where the prediction target is multi-dimensional, i.e., $\mathcal{Y} = \mathbb{R}^q$ with $q > 1$. Wang et al. (2023) developed the `PCP` method, based on implicit conditional generative models (CGMs). These CGMs allow for the generation of samples from the conditional distribution without requiring an explicit closed-form expression. The `PCP` method constructs prediction sets as unions of balls, whose centers are generated from the CGM. However, in `PCP`, the radius of these balls is fixed across the space, which can introduce significant limitations. In regions with low variability, a fixed radius may result in over-coverage, while for highly dispersed conditional distributions, it may lead to under-coverage, failing to capture the full extent of the relevant space. We observed that the performance of `PCP` deteriorates as the number of balls increases, exacerbating the heteroscedasticity problem. This underscores the need for a more adaptive methodology that can dynamically adjust the size of prediction sets in response to local variability in the data.

Our work addresses these challenges through the following main **contributions**:

- We propose a new `CP`^{2} method for constructing conditional confidence sets that adapts to the local structure of the data distribution, capable of addressing both classical regression problems where $\mathcal{Y} = \mathbb{R}$ and more complex multi-dimensional prediction tasks where $\mathcal{Y} = \mathbb{R}^q$. Our approach is versatile in accommodating scenarios involving either an explicit conditional density estimator or an implicit generative model; see Section 2.
- We develop a theoretical framework to analyze the properties of the proposed `CP`^{2} method, establishing both its marginal and approximate conditional validity. Furthermore, we demonstrate that asymptotic conditional coverage is attainable under a weak consistency assumption on the predictive distribution; see Section 3.
- We demonstrate the effectiveness of the proposed method through a series of experiments on synthetic and real-world datasets. The results indicate that our approach consistently outperforms existing methods in terms of conditional coverage. Specifically, it excels in handling classical regression problems, effectively addressing multimodality, and proves robust in the more challenging setting of multidimensional prediction tasks; see Section 4.

2 THE CP^2 FRAMEWORK

Problem setup. We want to construct marginally valid predictive sets with approximate conditional validity. We follow the split-conformal approach to conformal inference (Papadopoulos et al., 2002; Papadopoulos, 2008; Romano et al., 2019; Kivaranovic et al., 2020). We split the data samples into two disjoint subsets, the training set $\mathcal{T} = \{(\tilde{X}_k, \tilde{Y}_k)\}_{k=1}^m$ and calibration set $\mathcal{C} = \{(X_k, Y_k)\}_{k=1}^n$. It is assumed that the training and calibration data are mutually independent and i.i.d. with distribution $\mathrm{P}_{X,Y}$ over the feature vectors $X \in \mathbb{R}^d$ and response variables $Y \in \mathcal{Y}$. The target set $\mathcal{Y}$ can be either finite or continuous. Our goal is to construct a prediction set $\mathcal{C}_\alpha(X_{n+1})$ that contains the response Y_{n+1} with probability close to $1-\alpha$, where $\alpha \in (0,1)$ is the user-specified confidence level.

Conditional distribution estimator. An estimator $\Pi_{Y|X}$ of the conditional probability $\mathrm{P}_{Y|X}$ is learnt using the training data. There is a rich body of research on nonparametric conditional density estimation, with the most common methods relying on smoothing techniques such as kernel smoothing and local polynomial fitting. An alternative approach involves transforming the conditional density estimation task into a regression problem, allowing the application of nonparametric regression methods to approximate the conditional density. More recently, generative methods leveraging deep neural networks have been developed for nonparametric conditional density estimation, which enable sampling from the conditional distribution; see Abadi et al. (2016); Zhou et al. (2021) for examples of these techniques. In the sequel, the choice of this algorithm is treated as a black box.

CP^2 framework. There are three main ingredients for our approach:

1. In classical conformal prediction methods, the shape of the prediction set is specified by the score function $V(x,y)$; see (1). The first element of our construction is a family of explicitly given confidence sets $\mathcal{R}_z(x;t)$ parameterized by $t \in \mathsf{T}$ where T is a subset of $\mathbb{R}$ and $z \in \mathcal{Z}$ auxiliary variables. The index set T can, in most cases, be taken as either $\mathsf{T} = \mathbb{R}$ or $\mathsf{T} = \mathbb{R}_+$. The key assumptions for the confidence set are as follows: (a) The size of $\mathcal{R}_z(x;t)$ increases with $t \in \mathsf{T}$ for any $z \in \mathcal{Z}$. In addition, by choosing a sufficiently large value of t, the entire output space $\mathcal{Y}$ can be covered. (b) There exists a form of continuity for $t \mapsto \mathcal{R}_z(x;t)$. In mathematical terms, the following assumption should hold:

   H 1. For any $(x,z) \in \mathbb{R}^d \times \mathcal{Z}$, the confidence sets $\{\mathcal{R}_z(x;t)\}_{t\in\mathsf{T}}$ are non-decreasing, $\Pi_{Y|X=x}(\cap_{t\in\mathsf{T}}\mathcal{R}_z(x;t)) = 0$, $\cup_{t\in\mathcal{T}}\mathcal{R}_z(x;t) = \mathcal{Y}$; in addition, for any $t \in \mathsf{T}$, $\cap_{t'>t}\mathcal{R}_z(x;t') = \mathcal{R}_z(x;t)$.

   Example 2.1. For instance, $\mathcal{R}(x;t)$ can be chosen as a ball centered around an estimate of conditional mean $\mathrm{P}_{Y|X}$ with radius t. There is no auxiliary variables then an we remove subscript z. Examples of confidence intervals specialized to the case where $\mathcal{Y} = \mathbb{R}$ are given in Table 1.

   Example 2.2. If the predictive distribution is multimodal, a ball centered around the predictive mean often fails to provide an informative prediction set. Ideally, $\mathcal{R}_z(x;t)$ should correspond to the set with the highest predictive density (HPD) of $\mathrm{P}_{Y|X}$. However, HPD regions are difficult to determine in practice, even when the conditional predictive density is available. Following Wang et al. (2023), we may define the prediction set as $\mathcal{R}_z(x;t) := \cup_{i=1}^M \mathrm{B}(y_i,t)$, and it depends on exogenous variables $z = (y_1,\ldots,y_M) \in \mathcal{Z}$, where each y_i is sampled conditionally independently from the conditional generative model $\Pi_{Y|X=x}$.

2. To localize conformal prediction methods, it is convenient to introduce a function $f_\tau(\lambda)$ parameterized by τ. Such function aims to transform the conformity score λ and was introduced (albeit in a slightly different form) in Deutschmann et al. (2023); Han et al. (2022). Examples of such a function are $f_\tau(\lambda) = \tau\lambda$ and $f_\tau(\lambda) = \tau + \lambda$. We assume that:

   H2. There exists $\varphi \in \mathsf{T}$ such that $\tau \in \mathsf{T} \mapsto f_\tau(\varphi)$ is increasing and bijective. In addition, $\lambda \in \mathsf{T} \mapsto f_\tau(\lambda)$ is increasing for any $\tau \in \mathsf{T}$.

   We define $\tau_{x,z}$ using the estimated predictive density $\Pi_{Y|X=x}$ according to

   $$\tau_{x,z} = \inf\left\{\tau \in \mathsf{T} \colon \Pi_{Y|X=x}(\mathcal{R}_z(x; f_\tau(\varphi))) \geq 1-\alpha\right\}. \tag{3}$$

   It is easily shown that for any $\alpha \in (0,1)$, $x \in \mathbb{R}^d$, $z \in \mathcal{Z}$, then $\tau_{x,z} \in \mathsf{T}$ and $\Pi_{Y|X=x}(\mathcal{R}_z(x; f_{\tau_{x,z}}(\varphi))) \geq 1-\alpha$; see Lemma A.3.

3. Finally, we need to introduce the conformity score for the considered setup. The natural choice is the minimal size of the set required to cover the observation y at the input x for the auxiliary variables z: $\lambda_{x,y,z} = \inf\{t \in \mathsf{T} \colon y \in \mathcal{R}_z(x;t)\}$.

Table 1: Confidence sets $\mathcal{R}(x;t)$ found in the literature and also discussed in Gupta et al. (2022).

Lei et al. (2018) $[\text{pred}(x) - t, \text{pred}(x) + t]$	Lei et al. (2018) $[\text{pred}(x) - t\sigma(x), \text{pred}(x) + t\sigma(x)]$	Kivaranovic et al. (2020) $(1+t)[q_{\alpha/2}(x), q_{1-\alpha/2}(x)] - tq_{1/2}(x)$
Chernozhukov et al. (2021) $[q_t(x), q_{1-t}(x)]$	Romano et al. (2019) $[q_{\alpha/2}(x) - t, q_{1-\alpha/2}(x) + t]$	Sesia & Candès (2020) $[q_{\alpha/2}(x), q_{1-\alpha/2}(x)] \pm t(q_{1-\alpha/2}(x) - q_{\alpha/2}(x))$

4. The resulting procedure works as follows. Let $\bar{\Pi}_{Z|X=x}$ be a Markov kernel from $\mathbb{R}^d$ to $\mathcal{Z}$: for each $x \in \mathbb{R}^d$, $\bar{\Pi}_{Z|X=x}$ define a probability distribution on $\mathcal{Z}$. For $k \in \{1, \dots, n\}$, we set $\bar{\tau}_k := \tau_{X_k,Z_k}$ and $\bar{\lambda}_k := \lambda_{X_k,Y_k,Z_k}$ where $\{Z_k\}_{k=1}^n$ are sampled conditionally independently from $\bar{\Pi}_{Z|X=X_k}$. Given $X_{n+1} \in \mathbb{R}^d$, we sample $Z_{n+1} \sim \bar{\Pi}_{Z|X=X_{n+1}}$ conditionally independently from $\{(X_k, Y_k, Z_k)\}_{k=1}^n$, and construct the resulting CP^2 prediction set as

$$\mathcal{C}_\alpha(X_{n+1}) = \mathcal{R}_{Z_{n+1}}\left(X_{n+1}; f_{\bar{\tau}_{n+1}}\left(Q_{1-\alpha}(\mu_n)\right)\right), \tag{4}$$

where $Q_{1-\alpha}(\mu_n)$ is the $1-\alpha$ quantile of the distribution μ_n, and is given by

$$\mu_n = \frac{1}{n+1}\sum_{k=1}^n \delta_{f^{-1}_{\bar{\tau}_k}(\bar{\lambda}_k)} + \frac{1}{n+1}\delta_\infty. \tag{5}$$

The transformation $\{v \mapsto f_\tau(v)\}_{\tau \in \mathsf{T}}$ balances the following two factors: (a) The optimal parameter $\lambda_{x,y,z}$ ensuring that y is included in the confidence set $\mathcal{R}_z(x; \lambda_{x,y,z})$; (b) The parameter $\tau_{x,z}$ obtained from the probabilistic model $\Pi_{Y|X=x}$.

We stress that CP^2 is a general framework that can be adapted to many choices for conditional predictive density estimates, constructing the family of confidence sets, and selecting the calibration function $f_\tau(\lambda)$. However, we start with the simple example that shows that CP^2 is more general than the classical split-conformal CP approach.

Simple example of CP^2. We begin with a simple application of CP^2 to highlight its differences from the basic conformal approach, with $\mathcal{Y} = \mathbb{R}$. The calibration sets are defined as: $\mathcal{R}(x;t) = \{y \in \mathcal{Y}\colon |y - \text{pred}(x)| \le t\}$ for $t \in \mathbb{R}_+$. There are no auxiliary variables z in this case, so we omit z from the notation. Assumption **H**1 is easily satisfied with $\mathsf{T} = \mathbb{R}_+$. We then take $f_\tau(\lambda) = \tau\lambda$, $\tau \in \mathbb{R}_+$ and $\varphi = 1$: **H**2 is also satisfied. Note that $f_\tau^{-1}(\lambda) = \lambda/\tau$ for $\tau \in \mathbb{R}_+^*$. Using the CP^2 approach, we find that $\lambda_{x,y} = |y - \text{pred}(x)|$, which corresponds to a standard conformity score. The classical conformal prediction method defines the $1-\alpha$ quantile based on the associated empirical measure $\nu_n = \frac{1}{n+1}\sum_{k=1}^n \delta_{\bar{\lambda}_k} + \frac{1}{n+1}\delta_\infty$, where $\bar{\lambda}_k = |Y_k - \text{pred}(X_k)|$. CP^2 differs from the basic conformal approach by introducing $\tau_x = \arg\min\{\tau \in \mathsf{T}\colon \Pi_{Y|X=x}([\text{pred}(x) \pm \tau]) \ge 1-\alpha\}$ as in (3), where $[\text{pred}(x) \pm \tau] = [\text{pred}(x) - \tau, \text{pred}(x) + \tau]$. The prediction set becomes $[\text{pred}(x) \pm f_{\tau_x}(Q_{1-\alpha}(\mu_n))]$, where $\mu_n = \frac{1}{n+1}\sum_{k=1}^n \delta_{\bar{\lambda}_k/\tau_k} + \frac{1}{n+1}\delta_\infty$. In this setting, the choice of φ is irrelevant. Take $\varphi > 0$ and denote $\tau_x^\varphi = \arg\min\{\tau \in \mathsf{T}\colon \Pi_{Y|X=x}([\text{pred}(x) \pm f_\tau(\varphi)]) \ge 1-\alpha\}$. It is easily seen that $\tau_x^\varphi = \tau_x/\varphi$. The prediction set becomes $[\text{pred}(x) \pm f_{\tau_x^\varphi}(Q_{1-\alpha}(\mu_n^\varphi))]$, where $\mu_n^\varphi = \frac{1}{n+1}\sum_{k=1}^n \delta_{\bar{\lambda}_k/\bar{\tau}_k^\varphi} + \frac{1}{n+1}\delta_\infty$ with $\bar{\tau}_k^\varphi = \tau_{X_k}^\varphi$. Note that $Q_{1-\alpha}(\mu_n^\varphi) = \varphi Q_{1-\alpha}(\mu_n)$ and thus $f_{\tau_x^\varphi}(Q_{1-\alpha}(\mu_n^\varphi)) = f_{\tau_x}(Q_{1-\alpha}(\mu_n))$ showing that, the prediction set does not depend on the choice of φ. To illustrate the advantage of our method, in Figure 1 we present the prediction sets obtained with the classical CP method and CP^2 in the case of a Neal's funnel-shaped distribution in 2 dimensions; see Neal (2003, Section 9).

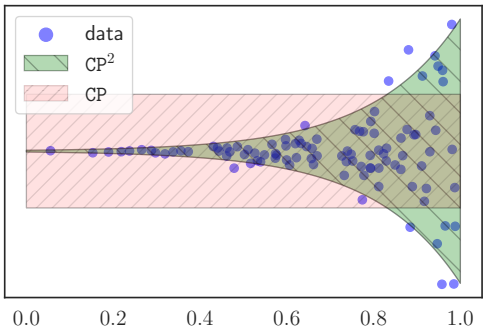

Figure 1: Predictions sets obtained via the standard CP and CP^2 methods.

The natural approach for the general case is to use the conditional distribution $\Pi_{Y|X=x}$ or its estimate to find Highest Predictive Density (HPD) regions and calibrate their size with the help of CP^2. We develop the respective general algorithm CP^2-HPD in Appendix C.1. However, the procedures to find HPDs are usually highly non-trivial and we only investigate this approach experimentally for

Algorithm 1 CP^2-PCP

Input: dataset $\{(X_k, Y_k)\}_{k\in[n]}$, significance level α, conditional distribution $\Pi_{Y|X}$, function f_t.
// Compute the $(1-\alpha)$-quantile
for $k = 1$ **to** n **do**
  Sample $\{\hat{Y}_{k,i}\}_{i=1}^{M}$ and $\{\tilde{Y}_{k,j}\}_{j=1}^{\tilde{M}}$ from $\Pi_{Y|X=X_k}$
  Set $\bar{\lambda}_k = \min_{i=1}^{M} \|Y_k - \hat{Y}_{k,i}\|$
  Set $\bar{\tau}_k = (t \mapsto f_t(\varphi))^{-1}\{Q_{1-\alpha}(\tilde{M}^{-1}\sum_{j=1}^{\tilde{M}} \delta_{\min_{i=1}^{M}\|\tilde{Y}_{k,j}-\hat{Y}_{k,i}\|})\}$
$Q_{1-\alpha}(\mu_n) \leftarrow \lceil (1-\alpha)(n+1)\rceil$-th smallest value in $\{f_{\bar{\tau}_k}^{-1}(\bar{\lambda}_k)\}_{k\in[n]} \cup \{\infty\}$
// Compute the prediction set for a new point $x \in \mathbb{R}^d$
Sample $z = \{\hat{Y}_i\}_{i=1}^{M}$ and $\{\tilde{Y}_j\}_{j=1}^{\tilde{M}}$ from $\Pi_{Y|X=x}$
Set $\tau_{x,z} = (t \mapsto f_t(\varphi))^{-1}\{Q_{1-\alpha}(\tilde{M}^{-1}\sum_{j=1}^{\tilde{M}} \delta_{\min_{i=1}^{M}\|\tilde{Y}_j-\hat{Y}_i\|})\}$
Output: $\mathcal{C}_\alpha(x) = \cup_{i=1}^{M} \mathrm{B}(\hat{Y}_i, f_{\tau_{x,z}}(Q_{1-\alpha}(\mu_n)))$.

synthetic data; see Section 4.1. Next, we provide a specific implementation of our general CP^2 framework that is universally applicable.

CP^2 with Implicit Conditional Generative Model: CP^2-PCP. We also develop a second instance of the CP^2 algorithm, inspired by Wang et al. (2023). Unlike CP^2-HPD, this approach does not require the conditional density. It is designed for cases where the conditional generative model (CGM) $\Pi_{Y|X}$ is implicit: we cannot evaluate it pointwise while being able to sample from it. For each calibration point X_k, we draw M random variables $\{\hat{Y}_{k,i}\}_{i=1}^{M}$ from $\Pi_{Y|X=X_k}$. We denote $Z_k = (\hat{Y}_{k,1}, \ldots, \hat{Y}_{k,M})$ and consider the confidence sets as the union of balls centered around the sample points $\mathcal{R}_{Z_k}(X_k; t) = \cup_{i=1}^{M} \mathrm{B}(\hat{Y}_{k,i}, t)$. With such choice, we get $\bar{\lambda}_k = \min_{i=1}^{M} \|Y_k - \hat{Y}_{k,i}\|$. We then draw a second sample $\{\tilde{Y}_{k,j}\}_{j=1}^{\tilde{M}}$, and compute $\bar{\tau}_k = \{t \in \mathbb{R}_+ \colon \tilde{M}^{-1}\sum_{j=1}^{\tilde{M}} \mathbb{1}_{\mathcal{R}_{Z_k}(X_k; f_t(\varphi))}(\tilde{Y}_{k,j}) \geq 1-\alpha\}$. It is easily seen that

$$\bar{\tau}_k = (t \mapsto f_t(\varphi))^{-1}\left\{Q_{1-\alpha}\left(\tfrac{1}{\tilde{M}}\sum_{j=1}^{\tilde{M}} \delta_{\min_{i=1}^{M}\|\tilde{Y}_{k,j}-\hat{Y}_{k,i}\|}\right)\right\}.$$

Given a new input $X_{n+1} \in \mathbb{R}^d$, we sample $Z_{n+1} = (\hat{Y}_{n+1,1}, \ldots, \hat{Y}_{n+1,M})$ and obtain prediction set as follows

$$\mathcal{C}_\alpha(X_{n+1}) = \left\{y \in \mathcal{Y} \colon \min_{i=1}^{M} \|y - \hat{Y}_{n+1,i}\| \leq f_{\bar{\tau}_{n+1}}(Q_{1-\alpha}(\mu_n))\right\},$$

where μ_n is given in (5). The CP^2-PCP method employs the same confidence set $\mathcal{R}_z(x; t)$ as the one used by PCP. This method effectively captures multimodalities using balls centered at likely outputs $\hat{Y}_{n+1,i}$. Furthermore, the conformity scores used by PCP correspond to our $\lambda_{x,y,z}$. However, the key distinction between the two algorithms lies in the additional parameter $\tau_{x,z}$ for CP^2-PCP, which requires the generation of a second random sample from $\Pi_{Y|X=x}$. This method is especially useful when solving equation (3) is intractable. We summarize CP^2-PCP in Algorithm 1.

3 Theoretical Guarantees

In this section, we provide both marginal and conditional guarantees for the prediction set $\mathcal{C}_\alpha(x)$ given in (4). The validity of these guarantees is ensured by the exchangeability of the calibration data, with the exception of Theorem 3.3 which relies on a concentration inequality and thus requires i.i.d. calibration data.

The following theorem establishes **marginal validity** of the predictive set defined by CP^2.

Theorem 3.1. *Assume **H1**-**H2**. Then, for any $\alpha \in (0,1)$, it holds $1-\alpha \leq \mathbb{P}(Y_{n+1} \in \mathcal{C}_\alpha(X_{n+1}))$. Moreover, if the conformity scores $\{f_{\bar{\tau}_k}^{-1}(\bar{\lambda}_k)\}_{k=1}^{n+1}$ are almost surely distinct, then it also holds that $\mathbb{P}(Y_{n+1} \in \mathcal{C}_\alpha(X_{n+1})) < 1-\alpha+(n+1)^{-1}$.*

The proof is postponed to Appendix A.1. Moreover, the upper bound on the coverage always holds when the distribution of $f^{-1}_{\bar{\tau}_k}(\bar{\lambda}_k)$ is continuous.

Now, we will investigate the **conditional validity**. Denote by $\mathrm{d_{TV}}$ the total variation distance and by $\mathbb{P}^{\mathcal{T}}$ the conditional probability given the training data.

Theorem 3.2. *Assume **H1**-**H2**, and let $\alpha \in (0,1)$. For any $x \in \mathbb{R}^d$ and $z \in \mathcal{Z}$, it holds*

$$\mathbb{P}^{\mathcal{T}}\left(Y_{n+1} \in \mathcal{C}_\alpha(x) \mid (X_{n+1}, Z_{n+1}) = (x,z)\right) \geq 1 - \alpha - \mathrm{d_{TV}}(\mathrm{P}_{Y|X=x}; \Pi_{Y|X=x}) - p^{(x,z)}_{n+1},$$

where $p^{(x,z)}_{n+1} = \mathbb{P}^{\mathcal{T}}\left(Q_{1-\alpha}(\mu_n) < f^{-1}_{\bar{\tau}_{n+1}}(\bar{\lambda}_{n+1}) \leq \varphi \,|\, (X_{n+1}, Z_{n+1}) = (x,z)\right)$.

The proof is postponed to Appendix A.1. The more accurately the estimator $\Pi_{Y|X=x}$ approximates the true conditional distribution, the closer the result will be to $1-\alpha$. The second term in the lower bound is $p^{(x,z)}_{n+1}$. Its expected value is upper bounded by $\mathbb{E}[p^{(X,Z)}_{n+1}] \leq \alpha$, and non-asymptotic bounds for this error term are developed in Appendix A.2.

Oracle asymptotic conditional coverage. We will now briefly discuss the asymptotic conditional coverage guarantee; details are provided in the supplementary paper. Assuming the availability of an oracle for the predictive distribution, i.e., $\mathrm{P}_{Y|X=x} = \Pi_{Y|X=x}$,we get under **H**1 and **H**2, that for any $t \in \mathbb{R}$,

$$\begin{aligned}\mathbb{P}\left(\lambda_{X,Y,Z} \leq f_{\tau_{X,Z}}(t) \,|\, X = x, Z = z\right) &= \mathbb{P}\left(Y \in \mathcal{R}_z(x; f_{\tau_{x,z}}(t)) \,|\, X = x, Z = z\right) \\ &= \Pi_{Y|X=x}\left(\mathcal{R}_z(x; f_{\tau_{x,z}}(t))\right),\end{aligned}$$

where (X,Y,Z) follows the same distribution than (X_k, Y_k, Z_k), $k \in \{1,\ldots,n\}$. Note that $\Pi_{Y|X=x}(\mathcal{R}_z(x; f_{\tau_{x,z}}(t))) \geq 1-\alpha$ if and only if $t \geq \varphi$, which implies that

$$\mathbb{P}(f^{-1}_{\tau_{X,Z}}(\lambda_{X,Y,Z}) \leq t \mid (X,Z) = (x,z)) \geq 1-\alpha \quad \text{if and only if} \quad t \geq \varphi. \tag{6}$$

From (6) it is easily seen that the $(1-\alpha)$-quantile of $f^{-1}_{\tau_{X,Z}}(\lambda_{X,Y,Z})$ is φ. The Glivenko–Cantelli Theorem (Van der Vaart, 2000, Theorem 19.1) demonstrates that $\sup_{t\in\mathbb{R}} |\mu_n(-\infty, t] - \mathbb{P}(f^{-1}_{\tau_{X,Z}}(\lambda_{X,Y,Z}) \leq t)| \to 0$ almost surely as $n \to \infty$, where μ_n is defined in (5). Since the convergence of the c.d.f. implies the convergence of the quantile function (Van der Vaart, 2000, Lemma 21.2), we deduce that $Q_{1-\alpha}(\mu_n) \to \varphi$ almost-surely as $n \to \infty$. Under weak additional conditions this implies that $\lim_{n\to\infty} p^{(x,z)}_{n+1} = 0$, $\bar{\Pi}_{Z|X} \times \mathrm{P}_X$-almost everywhere, where $\bar{\Pi}_{Z|X}$ is the Markov kernel used to draw the auxiliary variables z; see Appendix A.4. In this case, Theorem 3.1 implies the asymptotic validity of $\texttt{CP}^2$.

Asymptotic conditional coverage for $\texttt{CP}^2$. In practice, the oracle is unavailable. In the following theorem, we examine the asymptotic conditional conformal validity as the size of the training dataset, m_n, goes to infinity with n. In most cases, $\lim_{n\to\infty} m_n/n = \gamma > 0$, but this is not required here. To make the dependency of the estimator on the size of the training set explicit, we will denote the conditional distribution a $\Pi^{(m_n)}_{Y|X}$. Consider the following assumption.

H3. There exists sequence (r_n) such that $\lim_{n\to\infty} \mathbb{P}(\mathrm{d_{TV}}(\mathrm{P}_{X,Y}; \mathrm{P}_X \times \Pi^{(m_n)}_{Y|X}) \leq r_n) = 1$.

In most interesting case, we have $\lim_{n\to\infty} r_n = 0$. Such types of bounds can be deduced from Devroye & Lugosi (2001, Chapter 9). Let (X,Y,Z) and $(X,\hat{Y},Z)$ be random variables distributed according to $\mathrm{P}_{X,Y} \times \bar{\Pi}_{Z|X}$ and $\mathrm{P}_X \times \Pi^{(m_n)}_{Y|X} \times \bar{\Pi}_{Z|X}$, respectively.

Theorem 3.3. *Assume **H1**-**H2**-**H3** hold. If the distributions of $f^{-1}_{\tau_{X,Z}}(\lambda_{X,Y,Z})$ and $f^{-1}_{\tau_{X,Z}}(\lambda_{X,\hat{Y},Z})$ are continuous, then, it holds*

$$\left|\mathbb{P}^{\mathcal{T}}\left(Y_{n+1} \in \mathcal{C}_\alpha(X_{n+1}) \,|\, X_{n+1}, Z_{n+1}\right) - 1 + \alpha\right| = \mathrm{O}_{\mathbb{P}}\left(\sqrt{n^{-1}\log n} + r_n\right).$$

In Lei et al. (2018); Izbicki et al. (2020); Sesia & Candès (2020), the asymptotic conditional validity is demonstrated by assuming the consistency of their methods' estimators. For instance, Romano et al. (2019) assume that the conditional quantile regressor converges in L^2 towards the true quantile with high probability.

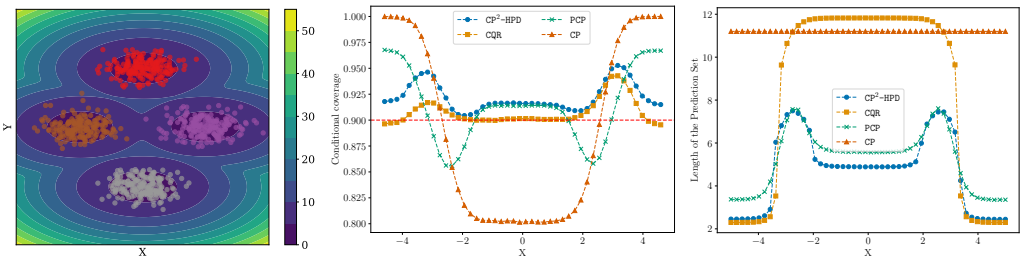

(a) Data and MDN estimate (b) Conditional coverage (c) Length of the prediction set

Figure 2: Mixture Density Network: the multimodal case.

4 Numerical Experiments

In this section, we conduct a comprehensive analysis demonstrating the advantage of CP^2 compared to standard and adaptive split conformal algorithms. Specifically, we benchmark our algorithm against several state-of-the-art methods: Conformalized Quantile Regression (Romano et al., 2019), Conformalized Histogram Regression (Sesia & Romano, 2021) and Probabilistic Conformal Prediction (Wang et al., 2023). All these method share some key aspects: they are built on top of the pre-trained models and do not require access to training data or the model's internals on both calibration and prediction steps. We aim to answer these specific questions: how does CP^2 performs in terms of coverage, conditional coverage and predictive set volume when compared to state-of-the-art methods on synthetic and real data.

4.1 Synthetic Data Experiment

In this example, (X_k, Y_k) is sampled from a mixture of $P = 4$ Gaussians; see Figure 2a. The number of training and calibration samples is $m = 10^4$ and $n = 10^3$, respectively. We fit a Mixture Density Network (MDN) as an explicit generative model, $\gamma_{Y|X=x}(y) = \sum_{\ell=1}^{P} \pi_\ell(x)\mathcal{N}(y; \mu_\ell(x), \sigma_\ell^2(x))$, where $\mu_\ell(\cdot)$, $\sigma_\ell(\cdot)$ and $\pi_\ell(\cdot)$ are all modeled by fully connected 2-layers neural networks (the condition $\sum_{\ell=1}^{P} \pi_\ell(x) = 1$ is ensured by using softmax activation functions). We use CP^2−HPD (the calculation of the HPD rates as well as τ_x and $\lambda_{x,y}$ is explicit in this case) with $f_t(v) = tv$. The parameters of the MDN are trained by maximizing the likelihood on the training set.

We compare the plain CP^2−HPD, PCP (with the same MDN as CP^2−HPD and $M = 50$ draws) and CQR. All methods achieve the desired marginal coverage $1 - \alpha = 0.9$. We illustrate the conditional coverage in Figure 2b and the lengths of the predictive sets in Figure 2c. CP with a fixed-width predictive set performs poorly in this multimodal example, both in terms of the size of the confidence set and the conditional coverage CP^2−HPD and CQR perform similarly in terms of conditional coverage (which remains close to $1 - \alpha = 0.9$). The conditional coverage of PCP varies between 0.85 and 0.95. CP^2−HPD produces shorter prediction sets compared to CQR and PCP. This is because CP^2−HPD uses an HPD confidence set that is more suitable for multimodal applications than the interval produced by CQR.

4.2 Real-world Regression Data Experiments

Datasets. We use publicly available regression datasets, which are also considered in Romano et al. (2019); Wang et al. (2023). Some of them come from the UCI repository: bike sharing (bike), protein structure (bio), blog feedback (blog), Facebook comments (fb1 and fb2). Other datasets come from US Department of Health surveys (meps19, meps20 and meps21), and from weather forecasts (temp; Cho et al. (2020)).

Methods. We compare the proposed CP^2−PCP method with Probabilistic Conformal Prediction (PCP; Wang et al. (2023)), Conformalized Quantile Regression (CQR; Romano et al. (2019)), Conformalized Histogram Regression (CHR; Sesia & Romano (2021)), Conformal Prediction with Conditional Guaranties (CPCG; Gibbs et al. (2023)), Localized Conformal Prediction (LCR; Guan (2023)). We also consider CQR2 which is a modification of CQR that uses inverse quantile as confor-

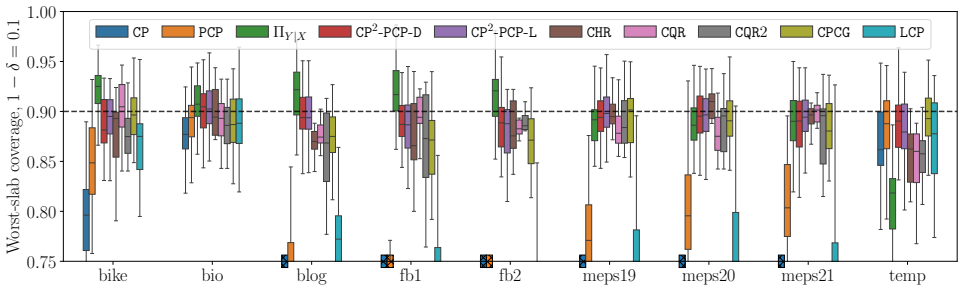

Figure 3: Worst-slab coverage on real data. Results averaged over 50 random splits of each dataset. Calibration and test set sizes set to 2000, 50 conditional samples for PCP, CP^2 and $\Pi_{Y|X}$. Worst-slab coverage parameter $(1-\delta)=0.1$. Nominal coverage level is $(1-\alpha)=0.9$ and is shown in dashed black. Methods with conditional coverage below 0.75 shown as cross-hatched on horizontal axis.

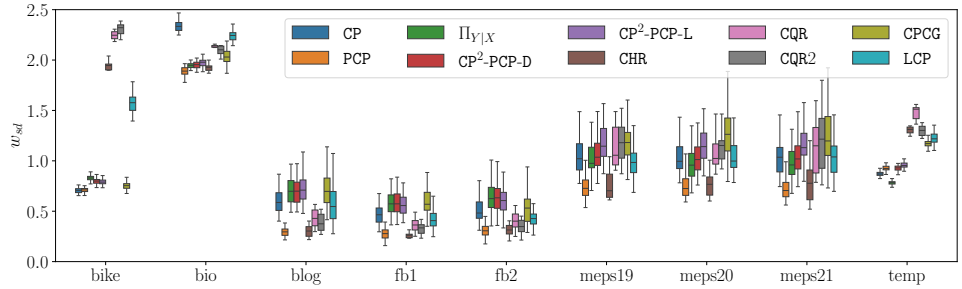

Figure 4: Sizes of the prediction sets on real data. We divide the size of the set by the standard deviation of response to present the results on the same scale.

mity score. For our method and PCP we use a Mixture Density Network (Bishop, 1994) to estimate the conditional distribution $\mathrm{P}_{Y|X}$, since it was chosen in Wang et al. (2023) as best-performing. We also consider different choices of f_t for our method: CP^2-PCP-L stands for CP^2-PCP with $f_t(v) = tv$ and CP^2-PCP-D stands for CP^2-PCP with $f_t(v) = t + v$. Our implementation of CP^2-PCP is summarized in Algorithm 1. Additionally, we consider $\Pi_{Y|X}$ which is a special case of CP^2-PCP with $f_t(v) = t$.

Metrics. Empirical coverage (marginal and conditional) is the main quantity of interest for prediction sets. We evaluate worst-slab conditional coverage (Cauchois et al., 2020; Romano et al., 2020b) in our experiments, see details in Appendix B.2. We also measure the total size of the predicted sets, scaled by the standard deviation of the response Y.

Experimental setup. Our experimental setup largely follows the approach outlined in Wang et al. (2023). Specifically, we split each dataset into training, calibration, and testing sets. A Mixture Density Network (MDN) with 10 components is then trained to approximate the conditional distribution $\mathrm{P}_{Y|X}$. For each calibration and test point, we first compute the Gaussian Mixture parameters, forming $\Pi_{Y|X}$, and subsequently draw $M = 5, 20, 50$ samples from these distributions, which yield $\mathcal{R}_z(x, t)$. This process is repeated across 50 different random splits of each dataset.

Results of the experiments for $M = 50$ samples are presented in Figures 3 and 4, additional results are available in Appendix B. In terms of marginal coverage, all methods achieve the target $1-\alpha$ value, except for $\Pi_{Y|X}$.

Standard conformal prediction fails to maintain the conditional coverage as expected. We can also observe that PCP consistently struggles with conditional coverage. On all the datasets CP^2-PCP provides valid conditional coverage, while CQR fails on blog and temp. CHR method shows unstable performance not achieving conditional coverage more often than other methods but sometimes providing narrower predictions sets. Additionally, CP^2-PCP significantly outperforms quantile regression-based methods in terms of size of the prediction sets on bike, bio and temp datasets. CPCG is a strong baseline, but our method shows better performance still. For example, on blog, fb1 and f2 datasets conditional coverage of CP^2-PCP is close to nominal, while prediction set size

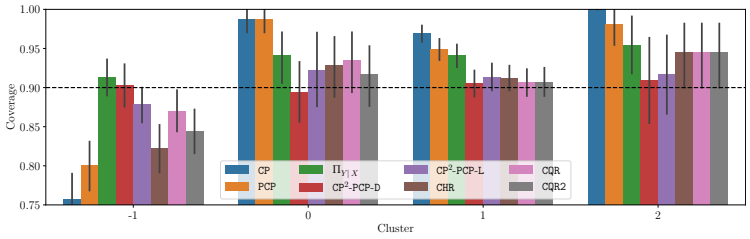

Figure 5: Conditional coverage for different clusters, `fb1` dataset. We have used HDBSCAN algorithm with minimum cluster size of 100, `min_samples` hyper-parameter of 20 and l_2 metric. Cluster label -1 corresponds to the outliers. Sample size for sampling-based methods was set to 50. Nominal coverage equals $(1-\alpha) = 0.9$ and is shown by a dashed black line.

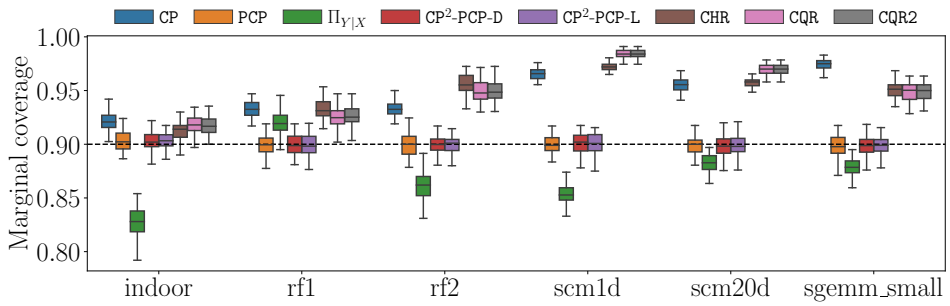

Figure 6: Marginal coverage for multi-target datasets, 50 replications. Sample size was set to 1000. Nominal coverage equals $(1-\alpha) = 0.9$ and is shown by a dashed black line.

are roughly the same between two methods. On `meps` datasets, conditional coverage is close, while the `CP`^{2}`-PCP` sets are smaller. Computational complexity of the prediction is the highest for `CPCG`, about 10 times that of our approach. `LCP` shows significantly lower conditional coverage than most methods on larger datasets.

Finally, we assess conditional coverage with the help of clustering. We apply HDBSCAN (Campello et al., 2013; McInnes & Healy, 2017) method to cluster the test set and then compute coverage within clusters. Results for `fb1` dataset are presented in Figure 5. We again observe that `CP` and `PCP` do not achieve conditional coverage and `CHR` and `CQR` performance is unstable. `CP`^{2}`-PCP` on the other hand maintains valid conditional coverage on all clusters and even on outliers (cluster label -1). Note that these are all outliers combined and they may not lie in the same region of the input space.

4.3 Real-world Regression Data with Multi-dimensional Targets

We also study `CP2` family of algorithms on the multi-target regression problems. Since selecting the threshold τ for our methods is not dependent on the number of dimensions in Y their application is straightforward. On the other hand, most other methods are inherently one-dimensional thus require the use of the Bonferroni correction (Dunn, 1961). Each coordinate is treated independently with miscoverage level adjusted to α/d, where d is the number of targets. As a result, for quantile regression-based methods prediction sets are rectangular cuboids, formed as a product of the corresponding intervals.

Datasets. We consider open-source multidimensional regression datasets: river flow data `rf1` and `rf2` (Xioufis et al., 2012), supply chain management `scm1d` and `scm20d` (Xioufis et al., 2012), indoor localisation `indoor` (Torres-Sospedra et al., 2014), GPU computation time `sgemm_small`[1] (Ballester-Ripoll et al., 2017).

[1]The full dataset contains 241600 examples. Due to computational constraints we randomly subsample 10000 examples for each replication of our experiment.

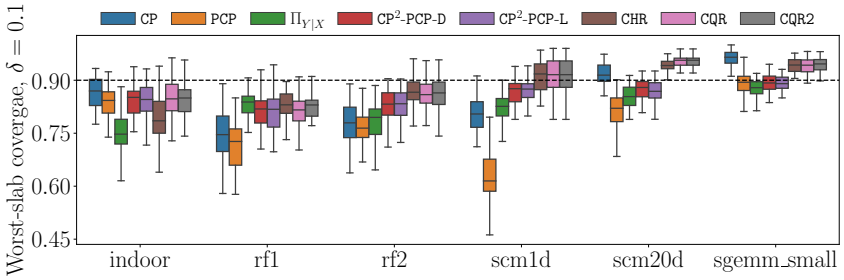

Figure 7: Conditional coverage for multi-target datasets targets, 50 replications. Sample size was set to 1000. Nominal coverage equals $(1 - \alpha) = 0.9$ and is shown in dashed black. Worst-slab coverage parameter $(1 - \delta) = 0.1$.

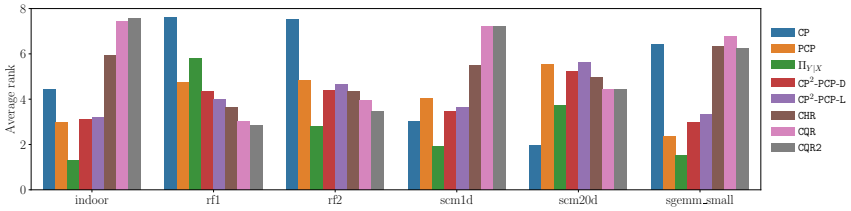

Figure 8: Average rank of the projected set size. For each pair of targets area of the corresponding 2D projection of the prediction set is calculated. For each test point and each pair of targets methods are ranked. Lower rank is smaller area. This graph shows averaged results of 10 replications.

We use the same **metrics** as before: marginal coverage and worst-slab coverage. Evaluating the difference in prediction set size is more complex in case of multiple dimensions. Due to computational constraints we perform pairwise comparisons between our methods and selected baselines, measuring approximate areas of 2D projections of the prediction sets (Wang et al., 2023). These results can be found on Figure 8. We approximate areas using a grid and fewer samples.

Since our methods naturally extend beyond one dimension, the **experimental setup** is almost identical. We use the same underlying model for $\mathrm{P}_{Y|X}$, the prediction set is now a union of d-dimensional balls of the same radius around the sampled centers. The number of samples is increased to 1000.

Results. In Figure 6 we show marginal coverage attained by different algorithms. As expected, naive application of 1D techniques CQR, CQR2 and CHR to multiple outputs produces significant overcover. `PCP` and `CP`^{2} methods naturally extend to multidimensional targets and provide correct marginal coverage. In Figure 7 we present the conditional coverage estimates for multi-target datasets. `PCP` significantly undercovers on `rf1`, `rf2` and `scm1d` datasets, while `CP`^{2} comes very close to the nominal coverage of 0.9. In case of CQR, CQR2 and CHR, they still overcover (`scm20d`, `sgemm`) or perform comparably to our approach. Figure 8 shows the aggregated results of the set size comparisons in multidimensional target setting. For each test point and each pair of axes we rank the methods by the area of the projection of the corresponding prediction set. The plot shows average rank for each method, aggregated across all axes pairs and replications. Lower rank corresponds to smaller area, which is our goal. For datasets `indoor`, `scm1d` and `sgemm_small` our approach performs better, while also providing sharper conditional covergae. On the remaining datasets `CP`^{2} performs similarly to the competitors.

5 Conclusion

We address the challenge of conditional coverage in CP, and overcome previous negative results by assuming the knowledge of a good estimator of $\mathrm{P}_{Y|X}$. Our proposed mechanism conformalized the conditional estimator $\Pi_{Y|X}$ to ensure marginal validity while maintaining similar conditional coverage guarantees. Specifically, if experts can provide an accurate conditional estimator, our algorithm `CP`^{2} generates nearly conditionally valid multidimensional prediction sets. This approach offers a practical solution for tackling heteroscedasticity in various machine learning applications.

REFERENCES

Martin Abadi, Andy Chu, Ian Goodfellow, H Brendan McMahan, Ilya Mironov, Kunal Talwar, and Li Zhang. Deep learning with differential privacy. In *Proceedings of the 2016 ACM SIGSAC conference on computer and communications security*, pp. 308–318, 2016.

Ahmed M Alaa, Zeshan Hussain, and David Sontag. Conformalized unconditional quantile regression. In *International Conference on Artificial Intelligence and Statistics*, pp. 10690–10702. PMLR, 2023.

Rafael Ballester-Ripoll, Enrique G. Paredes, and Renato Pajarola. Sobol tensor trains for global sensitivity analysis. *ArXiv*, abs/1712.00233, 2017. URL https://api.semanticscholar.org/CorpusID:22555685.

Christopher M Bishop. Mixture density networks. Technical Report. Aston University, Birmingham, 1994.

Stéphane Boucheron, Gábor Lugosi, and Olivier Bousquet. Concentration inequalities. In *Summer school on machine learning*, pp. 208–240. Springer, 2003.

T Tony Cai, Mark Low, and Zongming Ma. Adaptive confidence bands for nonparametric regression functions. *Journal of the American Statistical Association*, 109(507):1054–1070, 2014.

Ricardo J. G. B. Campello, Davoud Moulavi, and Jörg Sander. Density-based clustering based on hierarchical density estimates. In *Pacific-Asia Conference on Knowledge Discovery and Data Mining*, 2013. URL https://api.semanticscholar.org/CorpusID:32384865.

Maxime Cauchois, Suyash Gupta, and John C. Duchi. Knowing what you know: valid and validated confidence sets in multiclass and multilabel prediction. *J. Mach. Learn. Res.*, 22:81:1–81:42, 2020. URL https://api.semanticscholar.org/CorpusID:220496428.

Victor Chernozhukov, Kaspar Wüthrich, and Yinchu Zhu. Distributional conformal prediction. *Proceedings of the National Academy of Sciences*, 118(48):e2107794118, 2021.

Dongjin Cho, Cheolhee Yoo, Jungho Im, and Dong-Hyun Cha. Comparative assessment of various machine learning-based bias correction methods for numerical weather prediction model forecasts of extreme air temperatures in urban areas. *Earth and Space Science*, 7(4):e2019EA000740, 2020. doi: https://doi.org/10.1029/2019EA000740. URL https://agupubs.onlinelibrary.wiley.com/doi/abs/10.1029/2019EA000740.

Nicolas Deutschmann, Mattia Rigotti, and Maria Rodriguez Martinez. Adaptive conformal regression with jackknife+ rescaled scores. *arXiv preprint arXiv:2305.19901*, 2023.

Luc Devroye and Gábor Lugosi. *Combinatorial methods in density estimation*. Springer Science & Business Media, 2001.

Nicolas Dewolf, Bernard De Baets, and Willem Waegeman. Heteroskedastic conformal regression. *arXiv preprint arXiv:2309.08313*, 2023.

Olive Jean Dunn. Multiple comparisons among means. *Journal of the American Statistical Association*, 56(293):52–64, 1961. doi: 10.1080/01621459.1961.10482090. URL https://www.tandfonline.com/doi/abs/10.1080/01621459.1961.10482090.

Asaf Gendler, Tsui-Wei Weng, Luca Daniel, and Yaniv Romano. Adversarially robust conformal prediction. In *International Conference on Learning Representations*, 2021.

Isaac Gibbs, John J. Cherian, and Emmanuel J. Candès. Conformal prediction with conditional guarantees. *arXiv preprint arXiv:2305.12616*, 2023. URL https://arxiv.org/abs/2305.12616.

Leying Guan. Localized conformal prediction: A generalized inference framework for conformal prediction. *Biometrika*, 110(1):33–50, 2023.

Etash Kumar Guha, Shlok Natarajan, Thomas Möllenhoff, Mohammad Emtiyaz Khan, and Eugene Ndiaye. Conformal prediction via regression-as-classification. In *The Twelfth International Conference on Learning Representations*, 2024.

Chirag Gupta, Arun K Kuchibhotla, and Aaditya Ramdas. Nested conformal prediction and quantile out-of-bag ensemble methods. *Pattern Recognition*, 127:108496, 2022.

Xing Han, Ziyang Tang, Joydeep Ghosh, and Qiang Liu. Split localized conformal prediction. *arXiv preprint arXiv:2206.13092*, 2022.

Rohan Hore and Rina Foygel Barber. Conformal prediction with local weights: randomization enables robust guarantees. *Journal of the Royal Statistical Society Series B: Statistical Methodology*, pp. qkae103, 2024.

Rafael Izbicki, Gilson Shimizu, and Rafael Stern. Flexible distribution-free conditional predictive bands using density estimators. In *International Conference on Artificial Intelligence and Statistics*, pp. 3068–3077. PMLR, 2020.

Rafael Izbicki, Gilson Shimizu, and Rafael B Stern. Cd-split and hpd-split: Efficient conformal regions in high dimensions. *The Journal of Machine Learning Research*, 23(1):3772–3803, 2022.

Danijel Kivaranovic, Kory D Johnson, and Hannes Leeb. Adaptive, distribution-free prediction intervals for deep networks. In *International Conference on Artificial Intelligence and Statistics*, pp. 4346–4356. PMLR, 2020.

Shayan Kiyani, George Pappas, and Hamed Hassani. Conformal prediction with learned features. *arXiv preprint arXiv:2404.17487*, 2024.

Jing Lei and Larry Wasserman. Distribution-free prediction bands for non-parametric regression. *Journal of the Royal Statistical Society Series B: Statistical Methodology*, 76(1):71–96, 2014.

Jing Lei, Max G'Sell, Alessandro Rinaldo, Ryan J Tibshirani, and Larry Wasserman. Distribution-free predictive inference for regression. *Journal of the American Statistical Association*, 113(523): 1094–1111, 2018.

Michael Li, Matey Neykov, and Sivaraman Balakrishnan. Minimax optimal conditional density estimation under total variation smoothness. *Electronic Journal of Statistics*, 16(2):3937–3972, 2022.

Leland McInnes and John Healy. Accelerated hierarchical density based clustering. *2017 IEEE International Conference on Data Mining Workshops (ICDMW)*, pp. 33–42, 2017. URL https://api.semanticscholar.org/CorpusID:30310203.

Paul Melki, Lionel Bombrun, Boubacar Diallo, Jérôme Dias, and Jean-Pierre Da Costa. Group-conditional conformal prediction via quantile regression calibration for crop and weed classification. In *Proceedings of the IEEE/CVF International Conference on Computer Vision*, pp. 614–623, 2023.

Radford M Neal. Slice sampling. *The Annals of Statistics*, 31(3):705–767, 2003.

Harris Papadopoulos. Inductive conformal prediction: Theory and application to neural networks. In *Tools in artificial intelligence*. Citeseer, 2008.

Harris Papadopoulos, Kostas Proedrou, Volodya Vovk, and Alex Gammerman. Inductive confidence machines for regression. In *European Conference on Machine Learning*, pp. 345–356. Springer, 2002.

Yaniv Romano, Evan Patterson, and Emmanuel Candes. Conformalized quantile regression. *Advances in neural information processing systems*, 32, 2019.

Yaniv Romano, Rina Foygel Barber, Chiara Sabatti, and Emmanuel Candès. With malice toward none: Assessing uncertainty via equalized coverage. *Harvard Data Science Review*, 2(2):4, 2020a.

Yaniv Romano, Matteo Sesia, and Emmanuel Candes. Classification with valid and adaptive coverage. *Advances in Neural Information Processing Systems*, 33:3581–3591, 2020b.

Jonas Rothfuss, Fabio Ferreira, Simon Walther, and Maxim Ulrich. Conditional density estimation with neural networks: Best practices and benchmarks. *arXiv:1903.00954*, 2019.

Matteo Sesia and Emmanuel J Candès. A comparison of some conformal quantile regression methods. *Stat*, 9(1):e261, 2020.

Matteo Sesia and Yaniv Romano. Conformal prediction using conditional histograms. *Advances in Neural Information Processing Systems*, 34:6304–6315, 2021.

Glenn Shafer and Vladimir Vovk. A tutorial on conformal prediction. *Journal of Machine Learning Research*, 9(3), 2008.

Megh Shukla, Mathieu Salzmann, and Alexandre Alahi. Tic-tac: A framework for improved covariance estimation in deep heteroscedastic regression. In *Proceedings of the 41th International Conference on Machine Learning (ICML)*, Proceedings of Machine Learning Research. PMLR, 21–27 Jul 2024.

Joaquín Torres-Sospedra, Raúl Montoliu, Adolfo Martínez-Usó, Joan P. Avariento, Tomás J. Arnau, Mauri Benedito-Bordonau, and Joaquín Huerta. Ujiindoorloc: A new multi-building and multi-floor database for wlan fingerprint-based indoor localization problems. In *2014 International Conference on Indoor Positioning and Indoor Navigation (IPIN)*, pp. 261–270, 2014. doi: 10.1109/IPIN.2014.7275492.

Aad W Van der Vaart. *Asymptotic statistics*, volume 3. Cambridge university press, 2000.

Vladimir Vovk. Conditional validity of inductive conformal predictors. In *Asian conference on machine learning*, pp. 475–490. PMLR, 2012.

Vladimir Vovk, Alexander Gammerman, and Glenn Shafer. *Algorithmic learning in a random world*, volume 29. Springer, 2005.

Zhendong Wang, Ruijiang Gao, Mingzhang Yin, Mingyuan Zhou, and David Blei. Probabilistic conformal prediction using conditional random samples. In *International Conference on Artificial Intelligence and Statistics*, pp. 8814–8836. PMLR, 2023.

Eleftherios Spyromitros Xioufis, Grigorios Tsoumakas, William Groves, and Ioannis P. Vlahavas. Multi-target regression via input space expansion: treating targets as inputs. *Machine Learning*, 104:55 – 98, 2012. URL https://api.semanticscholar.org/CorpusID:1480930.

Xingyu Zhou, Yuling Jiao, Jin Liu, and Jian Huang. A deep generative approach to conditional sampling. *Journal of the American Statistical Association*, 118:1837 – 1848, 2021.

A Additional Results and Calculations

In this section, we analyze the theoretical results of Section 3. First, let's recall the definition of the quantile function for any distribution μ_n living in $\mathbb{R}$. For any $\alpha \in (0,1)$, the quantile $Q_{1-\alpha}(\mu_n)$ is defined by

$$Q_{1-\alpha}(\mu_n) = \inf\left\{t \in \mathbb{R} \colon \mu_n((-\infty, t]) \geq 1-\alpha\right\}.$$

Given a measure $\Pi_{Y|X=x}$ defined on $\sigma(\mathcal{Y})$, we consider for all $x \in \mathbb{R}^d$, $z \in \mathcal{Z}$, the parameters $\tau_{x,z}$ and $\lambda_{x,y,z}$ given by

$$\begin{aligned} \tau_{x,z} &= \inf\left\{\tau \in \mathsf{T} \colon \Pi_{Y|X=x}(\mathcal{R}_z(x; f_\tau(\varphi))) \geq 1-\alpha\right\}, \\ \lambda_{x,y,z} &= \inf\left\{\lambda \in \mathsf{T} \colon y \in \mathcal{R}_z(x;\lambda)\right\}, \end{aligned} \tag{7}$$

where φ is chosen as in **H**2, and by convention we set $\inf \emptyset = \infty$. We denote by δ_v the Dirac measure at $v \in \mathbb{R}$, and write $\bar{\tau}_k = \tau_{X_k,Z_k}$ and $\bar{\lambda}_k = \lambda_{X_k,Y_k,Z_k}$. In this Appendix, we study the coverage of the prediction set given $\forall (x,z) \in \mathbb{R} \times \mathcal{Z}$ by

$$\mathcal{C}_\alpha(x) = \mathcal{R}_z\left(x; f_{\tau_{x,z}}\left(Q_{1-\alpha}(\mu_n)\right)\right),$$

where the distribution μ_n is defined as

$$\mu_n = \frac{1}{n+1}\sum_{k=1}^{n}\delta_{f^{-1}_{\bar{\tau}_k}(\bar{\lambda}_k)} + \frac{1}{n+1}\delta_{\infty}.$$

The key idea behind the choice of $\bar{\tau}_k$ is to ensure that the conditional coverage of the prediction set $\mathcal{C}_\alpha(X_k)$ is approximately $1-\alpha$ when the empirical distribution $\Pi_{Y|X=X_k}$ is close to $\mathrm{P}_{Y|X=X_k}$. In other words, $\bar{\tau}_k$ is chosen such that the probability of the observed value Y_k given X_k falling inside the prediction set $\mathcal{C}_\alpha(X_k)$ is close to $1-\alpha$. On the other hand, the parameter $\bar{\lambda}_k$ is used to ensure that the prediction set $\mathcal{R}_{Z_k}(X_k;\bar{\lambda}_k)$ contains the observed value Y_k. Moreover, note that $\bar{\tau}_k$ only depends on the input data (X_k, Z_k), while $\bar{\lambda}_k$ depends on (X_k, Y_k, Z_k). Thus, the i.i.d. property of $\{(X_k, Y_k, Z_k)\colon k \in [n+1]\}$ ensures that the $\{(\bar{\tau}_k, \bar{\lambda}_k)\}_{k=1}^{n+1}$ are also i.i.d.

A.1 Proof of Theorems 3.1 and 3.2

Lemma A.1. *Assume **H1** hold. For any $(x, y, z) \in \mathbb{R}^d \times \mathcal{Y} \times \mathcal{Z}$, $\lambda_{x,y,z}$ exists in T, and we have $y \in \mathcal{R}_z(x; \lambda_{x,y,z})$.*

Proof. Let $(x, y, z) \in \mathbb{R}^d \times \mathcal{Y} \times \mathcal{Z}$ be fixed. Since $\cap_{t\in\mathsf{T}}\mathcal{R}_z(x;t) = \emptyset$ and $\cup_{t\in\mathsf{T}}\mathcal{R}_z(x;t) = \mathcal{Y}$, we deduce the existence of t_0 and t_1 such that $y \notin \mathcal{R}_z(x;t_0)$ and $y \in \mathcal{R}_z(x;t_1)$. Therefore, $\{t \in \mathsf{T}\colon y \in \mathcal{R}_z(x;t)\}$ is non-empty and lower-bounded by t_0. Thus, the infimum $\lambda_{x,y,z}$ exists. Now, let's prove that $y \in \mathcal{R}_z(x;\lambda_{x,y,z})$. Since $\lambda_{x,y,z} = \inf\{t \in \mathsf{T}\colon y \in \mathcal{R}_z(x;t)\}$, we deduce the existence of a decreasing sequence $\{\lambda_n\}_{n\in\mathbb{N}}$ such that $y \in \mathcal{R}_z(x;\lambda_n)$ and $\lim_{n\to\infty}\lambda_n = \lambda_{x,y,z}$. By definition of $\{\lambda_n\}_{n\in\mathbb{N}}$, we have $y \in \cap_{n\in\mathbb{N}}\mathcal{R}_z(x;\lambda_n)$. However, using **H1**, remark that

$$\begin{aligned}\cap_{n\in\mathbb{N}}\mathcal{R}_z(x;\lambda_n) &= \cap_{n\in\mathbb{N}}\cap_{t>\lambda_n}\mathcal{R}_z(x;t)\\ &= \cap_{t>\lim_{n\to\infty}\lambda_n}\mathcal{R}_z(x;t)\\ &= \cap_{t>\lambda_{x,y,z}}\mathcal{R}_z(x;t) = \mathcal{R}_z(x;\lambda_{x,y,z}).\end{aligned}$$

Since $y \in \cap_{n\in\mathbb{N}}\mathcal{R}_z(x;\lambda_n)$, it implies that $y \in \mathcal{R}_z(x;\lambda_{x,y,z})$. □

We will now present the proof for Theorem 3.1, which establishes the marginal validity of our proposed method.

Theorem A.2. *Assume **H1**-**H2** hold, if $\{f^{-1}_{\bar{\tau}_k}(\bar{\lambda}_k)\}_{k=1}^{n+1}$ are almost surely distinct, then it follows*

$$1-\alpha \le \mathbb{P}^{\mathcal{T}}\left(Y_{n+1} \in \mathcal{C}_\alpha(X_{n+1})\right) < 1-\alpha+\frac{1}{n+1}. \tag{8}$$

Proof. Using Lemma A.1, we have

$$\begin{aligned}\mathbb{P}^{\mathcal{T}}\left(Y_{n+1} \in \mathcal{C}_\alpha(X_{n+1})\right) &= \mathbb{P}^{\mathcal{T}}\left(Y_{n+1} \in \mathcal{R}_{Z_{n+1}}\left(X_{n+1}, f_{\bar{\tau}_{n+1}}(Q_{1-\alpha}(\mu_n))\right)\right)\\ &= \mathbb{P}^{\mathcal{T}}\left(\lambda_{n+1} \le f_{\bar{\tau}_{n+1}}(Q_{1-\alpha}(\mu_n))\right).\end{aligned}$$

Since $\lambda \mapsto f_{\bar{\tau}_{n+1}}(\lambda)$ is increasing by **H2**, we deduce that

$$\mathbb{P}^{\mathcal{T}}\left(\lambda_{n+1} \le f_{\bar{\tau}_{n+1}}(Q_{1-\alpha}(\mu_n))\right) = \mathbb{P}^{\mathcal{T}}\left(f^{-1}_{\bar{\tau}_{n+1}}(\lambda_{n+1}) \le Q_{1-\alpha}(\mu_n)\right).$$

Denote by $V_k = f^{-1}_{\bar{\tau}_k}(\bar{\lambda}_k)$, the exchangeability of the data $\{(X_k, Y_k, Z_k)\colon k \in [n+1]\}$ implies that

$$\begin{aligned}\mathbb{P}^{\mathcal{T}}\left(V_{n+1} \le Q_{1-\alpha}\left(\sum_{k=1}^{n}\frac{\delta_{V_k}}{n+1}+\frac{\delta_\infty}{n+1}\right)\right) &= \mathbb{P}^{\mathcal{T}}\left(V_{n+1} \le Q_{1-\alpha}\left(\sum_{k=1}^{n+1}\frac{\delta_{V_k}}{n+1}\right)\right)\\ &= \frac{1}{n+1}\sum_{k=1}^{n+1}\mathbb{E}^{\mathcal{T}}\left[\mathbb{1}_{V_k} \le Q_{1-\alpha}\left(\frac{1}{n+1}\sum_{k=1}^{n+1}\delta_{V_k}\right)\right]\\ &= \mathbb{E}^{\mathcal{T}}\left[\mathbb{E}^{\mathcal{T}}\left[\mathbb{1}_{V_I} \le Q_{1-\alpha}\left(\frac{1}{n+1}\sum_{k=1}^{n+1}\delta_{V_k}\right)\,\middle|\, V_1,\ldots,V_{n+1}\right]\right],\end{aligned}$$

where $I \sim \mathcal{U}nif(1, \ldots, n+1)$. Therefore, the definition of the quantile function implies the lower bound in (8). Moreover, if there are no ties between the $\{V_k\}_{k=1}^{n+1}$, then

$$\mathbb{P}^{\mathcal{T}}\left(f^{-1}_{\bar{\tau}_{n+1}}(\lambda_{n+1}) \leq Q_{1-\alpha}(\mu_n)\right) < 1 - \alpha + \frac{1}{n+1}.$$

□

The following lemma provides conditions under which $\Pi_{Y|X=x}(\mathcal{R}_z(x; f_{\tau_{x,z}}(\varphi))) \geq 1 - \alpha$.

Lemma A.3. *Assume **H**1-**H**2 hold, and let $\alpha \in (0,1)$, $x \in \mathbb{R}^d$, $z \in \mathcal{Z}$. If $\Pi_{Y|X=x}$ is a probability measure, then $\tau_{x,z}$ is defined in T and $\Pi_{Y|X=x}(\mathcal{R}_z(x; f_{\tau_{x,z}}(\varphi))) \geq 1 - \alpha$.*

Proof. Let $x \in \mathbb{R}^d$ be such that $\Pi_{Y|X=x}$ is a probability measure, and fix $z \in \mathcal{Z}$. Since $\tau \mapsto f_\tau(\varphi)$ is increasing and bijective by **H**2, we have

$$\begin{aligned}\sup_{\tau \in \mathsf{T}} \Pi_{Y|X=x}(\mathcal{R}_z(x; f_\tau(\varphi))) &= \Pi_{Y|X=x}\left(\cup_{\tau \in \mathsf{T}} \mathcal{R}_z(x; f_\tau(\varphi))\right) \\ &= \Pi_{Y|X=x}\left(\cup_{t \in \mathsf{T}} \mathcal{R}_z(x; t)\right) = 1.\end{aligned}$$

The previous equality shows the existence of $\tau \in \mathsf{T}$ such that $\Pi_{Y|X=x}(\mathcal{R}_z(x; f_\tau(\varphi))) \geq 1 - \alpha$. Therefore $\{\tau \in \mathsf{T} \colon \Pi_{Y|X=x}(\mathcal{R}_z(x; f_\tau(\varphi))) \geq 1 - \alpha\}$ is non-empty. This proves the existence of $\tau_{x,z} = \inf\{\tau \in \mathsf{T} \colon \Pi_{Y|X=x}(\mathcal{R}_z(x; f_\tau(\varphi))) \geq 1 - \alpha\}$ in $\mathsf{T} \cup \{-\infty\}$. Moreover, $\tau_{x,z} > -\infty$, otherwise we would have

$$1 - \alpha \leq \inf_{\tau \in \mathsf{T}} \Pi_{Y|X=x}(\mathcal{R}_z(x; f_\tau(\varphi))) = \Pi_{Y|X=x}\left(\cap_{t \in \mathsf{T}} \mathcal{R}_z(x; t)\right) = 0.$$

Therefore, we deduce that $\tau_{x,z} \in \mathsf{T}$. Lastly, remark that

$$\begin{aligned}\Pi_{Y|X=x}(\mathcal{R}_z(x; f_{\tau_{x,z}}(\varphi))) &= \Pi_{Y|X=x}(\cap_{\tau > \tau_{x,z}} \mathcal{R}_z(x; f_\tau(\varphi))) \\ &= \inf_{\tau > \tau_{x,z}} \Pi_{Y|X=x}(\mathcal{R}_z(x; f_\tau(\varphi))) \geq 1 - \alpha.\end{aligned}$$

□

Now, we prove Theorem 3.2. This result guarantees that the conditional confidence intervals constructed by our method approximately satisfy the desired coverage of $1-\alpha$. Given $(x, y) \in \mathbb{R}^d \times \mathcal{Z}$, let's introduce

$$\begin{aligned}p^{(x,z)}_{n+1} &= \mathbb{P}^{\mathcal{T}}\left(Q_{1-\alpha}(\mu_n) < f^{-1}_{\tau_{x,z}}\left(\lambda_{x,Y_{n+1},z}\right) \leq \varphi \,|\, X_{n+1} = x, Z_{n+1} = z\right), \\ q^{(x,z)}_{n+1} &= \mathbb{P}^{\mathcal{T}}\left(\varphi < f^{-1}_{\tau_{x,z}}\left(\lambda_{x,Y_{n+1},z}\right) \leq Q_{1-\alpha}(\mu_n) \,|\, X_{n+1} = x, Z_{n+1} = z\right).\end{aligned}$$

Theorem A.4. *Assume **H**1-**H**2 hold, let $x \in \mathbb{R}^d$ be such that $\Pi_{Y|X=x}$ is a probability measure. For any $z \in \mathcal{Z}$, it follows that*

$$\begin{aligned}1 - \alpha - \mathrm{d_{TV}}(\mathrm{P}_{Y|X=x}; \Pi_{Y|X=x}) - p^{(x,z)}_{n+1} &\leq \mathbb{P}^{\mathcal{T}}\left(Y_{n+1} \in \mathcal{C}_\alpha(X_{n+1}) \mid X_{n+1} = x, Z_{n+1} = z\right) \\ &\leq \Pi_{Y|X=x}(\mathcal{R}_z(x; f_{\tau_{x,z}}(\varphi))) + \mathrm{d_{TV}}(\mathrm{P}_{Y|X=x}; \Pi_{Y|X=x}) + q^{(x,z)}_{n+1}.\end{aligned}$$

Proof. First, recall that $\mathcal{C}_\alpha(x)$ is given in (4), and $\lambda_{x,Y_{n+1},z}$ is defined in (7). Applying Lemma A.1, we know that $\lambda_{x,Y_{n+1},z}$ is defined in T, and also that $Y_{n+1} \in \mathcal{R}_z(x; \lambda_{x,Y_{n+1},z})$. Hence, it holds

$$\begin{aligned}&\mathbb{P}^{\mathcal{T}}\left(Y_{n+1} \in \mathcal{C}_\alpha(X_{n+1}) \,|\, X_{n+1} = x, Z_{n+1} = z\right) \\ &\quad = \mathbb{P}^{\mathcal{T}}\left(Y_{n+1} \in \mathcal{R}_z\left(x; f_{\tau_{x,z}}(Q_{1-\alpha}(\mu_n))\right) \mid X_{n+1} = x, Z_{n+1} = z\right) \\ &\quad = \mathbb{P}^{\mathcal{T}}\left(\lambda_{x,Y_{n+1},z} \leq f_{\tau_{x,z}}\left(Q_{1-\alpha}(\mu_n)\right) \mid X_{n+1} = x, Z_{n+1} = z\right). \quad (9)\end{aligned}$$

Let's introduce the term $\mathbb{P}^{\mathcal{T}}(\lambda_{x,Y_{n+1},z} \leq f_{\tau_{x,z}}(\varphi) \,|\, X_{n+1} = x, Z_{n+1} = z)$ as follows:

$$\begin{aligned}\mathbb{P}^{\mathcal{T}}\left(\lambda_{x,Y_{n+1},z} \leq f_{\tau_{x,z}}\left(Q_{1-\alpha}(\mu_n)\right) \,|\, X_{n+1} = x, Z_{n+1} = z\right) \\ = \mathbb{P}^{\mathcal{T}}\left(\lambda_{x,Y_{n+1},z} \leq f_{\tau_{x,z}}\left(Q_{1-\alpha}(\mu_n)\right) \,|\, X_{n+1} = x, Z_{n+1} = z\right) \\ \pm \mathbb{P}^{\mathcal{T}}\left(\lambda_{x,Y_{n+1},z} \leq f_{\tau_{x,z}}(\varphi) \,|\, X_{n+1} = x, Z_{n+1} = z\right). \quad (10)\end{aligned}$$

Now, we will control the difference between the two terms of the previous equation. Let A and B be defined as

$$\begin{aligned}A &= \mathbb{P}^{\mathcal{T}}\left(f^{-1}_{\tau_{x,z}}(\lambda_{x,Y_{n+1},z}) \leq Q_{1-\alpha}(\mu_n) < \varphi \,|\, X_{n+1} = x, Z_{n+1} = z\right), \\ B &= \mathbb{P}^{\mathcal{T}}\left(f^{-1}_{\tau_{x,z}}(\lambda_{x,Y_{n+1},z}) \leq \varphi \leq Q_{1-\alpha}(\mu_n) \,|\, X_{n+1} = x, Z_{n+1} = z\right).\end{aligned}$$

We have

$$\begin{aligned}\mathbb{P}^{\mathcal{T}}\left(\lambda_{x,Y_{n+1},z} \leq f_{\tau_{x,z}}\left(Q_{1-\alpha}(\mu_n)\right) \,|\, X_{n+1} = x, Z_{n+1} = z\right) \\ = A + B + \mathbb{P}^{\mathcal{T}}\left(\varphi < f^{-1}_{\tau_{x,z}}\left(\lambda_{x,Y_{n+1},z}\right) \leq Q_{1-\alpha}(\mu_n) \,|\, X_{n+1} = x, Z_{n+1} = z\right),\end{aligned}$$

and also

$$\begin{aligned}\mathbb{P}^{\mathcal{T}}\left(\lambda_{x,Y_{n+1},z} \leq f_{\tau_{x,z}}(\varphi) \,|\, X_{n+1} = x, Z_{n+1} = z\right) \\ = A + B + \mathbb{P}^{\mathcal{T}}\left(Q_{1-\alpha}(\mu_n) < f^{-1}_{\tau_{x,z}}\left(\lambda_{x,Y_{n+1},z}\right) \leq \varphi \,|\, X_{n+1} = x, Z_{n+1} = z\right).\end{aligned}$$

Therefore, the difference between the terms introduced in (10) can be rewritten as

$$\begin{aligned}\mathbb{P}^{\mathcal{T}}\left(\lambda_{x,Y_{n+1},z} \leq f_{\tau_{x,z}}\left(Q_{1-\alpha}(\mu_n)\right) \,|\, X_{n+1} = x, Z_{n+1} = z\right) \\ - \mathbb{P}^{\mathcal{T}}\left(\lambda_{x,Y_{n+1},z} \leq f_{\tau_{x,z}}(\varphi) \,|\, X_{n+1} = x, Z_{n+1} = z\right) \\ = \mathbb{P}^{\mathcal{T}}\left(\varphi < f^{-1}_{\tau_{x,z}}\left(\lambda_{x,Y_{n+1},z}\right) \leq Q_{1-\alpha}(\mu_n) \,|\, X_{n+1} = x, Z_{n+1} = z\right) \\ - \mathbb{P}^{\mathcal{T}}\left(Q_{1-\alpha}(\mu_n) < f^{-1}_{\tau_{x,z}}\left(\lambda_{x,Y_{n+1},z}\right) \leq \varphi \,|\, X_{n+1} = x, Z_{n+1} = z\right). \quad (11)\end{aligned}$$

1. By definition of the total variation distance, we have

$$\begin{aligned}\mathbb{P}^{\mathcal{T}}\left(\lambda_{x,Y_{n+1},z} \leq f_{\tau_{x,z}}(\varphi) \,|\, X_{n+1} = x, Z_{n+1} = z\right) \\ \geq \mathbb{P}^{\mathcal{T}}\left(\lambda_{x,\hat{Y}_{n+1},z} \leq f_{\tau_{x,z}}(\varphi) \,|\, X_{n+1} = x, Z_{n+1} = z\right) - \mathrm{d_{TV}}(\mathrm{P}_{Y|X=x}; \Pi_{Y|X=x}).\end{aligned}$$

   Moreover, Lemma A.3 implies that

$$\begin{aligned}\mathbb{P}^{\mathcal{T}}\left(\lambda_{x,\hat{Y}_{n+1},z} \leq f_{\tau_{x,z}}(\varphi) \,|\, X_{n+1} = x, Z_{n+1} = z\right) \\ = \mathbb{P}^{\mathcal{T}}\left(\hat{Y}_{n+1} \in \left\{y \in \mathcal{Y} \colon \lambda_{x,y,z} \leq f_{\tau_{x,z}}(\varphi)\right\} \,|\, X_{n+1} = x, Z_{n+1} = z\right) \\ = \mathbb{P}^{\mathcal{T}}\left(\hat{Y}_{n+1} \in \mathcal{R}_z(x; f_{\tau_{x,z}}(\varphi)) \,|\, X_{n+1} = x, Z_{n+1} = z\right) \\ = \Pi_{Y|X=x}(\mathcal{R}_z(x; f_{\tau_{x,z}}(\varphi))) \geq 1 - \alpha.\end{aligned}$$

   Therefore, we deduce that

$$\mathbb{P}^{\mathcal{T}}\left(\lambda_{x,Y_{n+1},z} \leq f_{\tau_{x,z}}(\varphi) \,|\, X_{n+1} = x, Z_{n+1} = z\right) \geq 1 - \alpha - \mathrm{d_{TV}}(\mathrm{P}_{Y|X=x}; \Pi_{Y|X=x}).$$

   Combining the previous result with (10) and (11) shows that

$$\begin{aligned}\mathbb{P}^{\mathcal{T}}\left(\lambda_{x,Y_{n+1},z} \leq f_{\tau_{x,z}}\left(Q_{1-\alpha}(\mu_n)\right) \,|\, X_{n+1} = x, Z_{n+1} = z\right) \geq 1 - \alpha - \mathrm{d_{TV}}(\mathrm{P}_{Y|X=x}; \Pi_{Y|X=x}) \\ - \mathbb{P}^{\mathcal{T}}\left(Q_{1-\alpha}(\mu_n) < f^{-1}_{\tau_{x,z}}\left(\lambda_{x,Y_{n+1},z}\right) \leq \varphi \,|\, X_{n+1} = x, Z_{n+1} = z\right).\end{aligned}$$

   Finally, using (9) gives a lower bound on $\mathbb{P}^{\mathcal{T}}\left(Y_{n+1} \in \mathcal{C}_\alpha(X_{n+1}) \mid X_{n+1} = x, Z_{n+1} = z\right)$.

2. By definition of the total variation distance, we have

$$\mathbb{P}^{\mathcal{T}}\left(\lambda_{x,Y_{n+1},z} \leq f_{\tau_{x,z}}(\varphi) \,|\, X_{n+1}=x, Z_{n+1}=z\right) \leq \mathbb{P}^{\mathcal{T}}\left(\lambda_{x,\hat{Y}_{n+1},z} \leq f_{\tau_{x,z}}(\varphi) \,|\, X_{n+1}=x, Z_{n+1}=z\right) + \mathrm{d_{TV}}(\mathrm{P}_{Y|X=x}; \Pi_{Y|X=x}).$$

Moreover, Lemma A.3 implies that

$$\mathbb{P}^{\mathcal{T}}\left(\lambda_{x,\hat{Y}_{n+1},z} \leq f_{\tau_{x,z}}(\varphi) \,|\, X_{n+1}=x, Z_{n+1}=z\right) = \Pi_{Y|X=x}(\mathcal{R}_z(x; f_{\tau_{x,z}}(\varphi))).$$

Therefore, we deduce that

$$\mathbb{P}^{\mathcal{T}}\left(\lambda_{x,Y_{n+1},z} \leq f_{\tau_{x,z}}(\varphi) \,|\, X_{n+1}=x, Z_{n+1}=z\right) \leq \Pi_{Y|X=x}(\mathcal{R}_z(x; f_{\tau_{x,z}}(\varphi))) + \mathrm{d_{TV}}(\mathrm{P}_{Y|X=x}; \Pi_{Y|X=x}).$$

Finally, combining the previous result with (10) and (11) shows that

$$\mathbb{P}^{\mathcal{T}}\left(\lambda_{x,Y_{n+1},z} \leq f_{\tau_{x,z}}\left(Q_{1-\alpha}(\mu_n)\right) \,|\, X_{n+1}=x, Z_{n+1}=z\right) \leq \Pi_{Y|X=x}(\mathcal{R}_z(x; f_{\tau_{x,z}}(\varphi))) + \mathrm{d_{TV}}(\mathrm{P}_{Y|X=x}; \Pi_{Y|X=x}) + q_{n+1}^{(x,z)}.$$

□

A.2 Bound on $p_{n+1}^{(x,z)}$ and $q_{n+1}^{(x,z)}$

The objective of this section is to study the conditional guarantee obtained in Theorem A.4. Under some assumptions, we have demonstrated that the conditional coverage is controlled as follows:

$$1-\alpha-\mathrm{d_{TV}}(\mathrm{P}_{Y|X=x}; \Pi_{Y|X=x}) - p_{n+1}^{(x,z)} \leq \mathbb{P}^{\mathcal{T}}\left(Y_{n+1} \in \mathcal{C}_\alpha(X_{n+1}) \mid X_{n+1}=x, Z_{n+1}=z\right) \leq \Pi_{Y|X=x}(\mathcal{R}_z(x; f_{\tau_{x,z}}(\varphi))) + \mathrm{d_{TV}}(\mathrm{P}_{Y|X=x}; \Pi_{Y|X=x}) + q_{n+1}^{(x,z)},$$

In the following, we consider the cumulative density functions $F\colon t \mapsto \mathbb{P}^{\mathcal{T}}(f^{-1}_{\tau_{X,Z}}(\lambda_{X,Y,Z}) \leq t)$ and $\hat{F}\colon t \mapsto \mathbb{P}^{\mathcal{T}}(f^{-1}_{\tau_{X,Z}}(\lambda_{X,\hat{Y},Z}) \leq t)$, where $(X,Y,Z) \sim \mathrm{P}_X \times \mathrm{P}_{Y|X} \times \Pi_{Z|X}$ and $(X,\hat{Y},Z) \sim \mathrm{P}_X \times \Pi_{Y|X} \times \Pi_{Z|X}$. We denote by μ and $\hat{\mu}$ the law of the random variables $f^{-1}_{\tau_{X,Z}}(\lambda_{X,Y,Z})$ and $f^{-1}_{\tau_{X,Z}}(\lambda_{X,\hat{Y},Z})$. Moreover, recall that $\mu_n = \frac{1}{n+1}\sum_{k=1}^{n} \delta_{f^{-1}_{\bar{\tau}_{X_k}}(\bar{\lambda}_k)} + \frac{1}{n+1}\delta_\infty$. Note, the quantile $Q_{1-\alpha}(\mu_n)$ is an order statistic with a known distribution that converges to the true quantile $Q_{1-\alpha}(\mu)$. The quantile is defined for any $t \in (0,1)$ by

$$Q_t(\nu) = \inf\{u \in \mathbb{R}\colon \nu((-\infty,u]) \geq t\}, \qquad \text{where } \nu \in \{\mu, \mu_n, \hat{\mu}\}. \tag{12}$$

Theorem A.5. *Assume **H1**-**H2** hold, and let $x \in \mathbb{R}^d$ be such that $\Pi_{Y|X=x}$ is a probability measure. For any $\epsilon \in [0, 1-\alpha)$, if $p_\epsilon = \mathbb{P}^{\mathcal{T}}(f^{-1}_{\tau_{X,Z}}(\lambda_{X,Y,Z}) < Q_{1-\alpha-\epsilon}(\mu)) \leq 1-\alpha$, then it follows that*

$$p_{n+1}^{(x,z)} \leq \mathbb{P}^{\mathcal{T}}\left(Q_{1-\alpha-\epsilon}(\mu) < f^{-1}_{\tau_{x,y}}(\lambda_{x,Y_{n+1},z}) \leq Q_{1-\alpha}(\hat{\mu}) \,|\, X_{n+1}=x, Z_{n+1}=z\right) + \exp\left(-np_\epsilon(1-p_\epsilon)h\left(\frac{1-\alpha-p_\epsilon}{p_\epsilon(1-p_\epsilon)}\right)\right),$$

where $h : u \mapsto (1+u)\log(1+u) - u$.

Proof. Let $\epsilon \in [0, 1-\alpha)$, $x \in \mathbb{R}^d$, and consider

$$A = \{Q_{1-\alpha}(\mu_n) < Q_{1-\alpha-\epsilon}(\mu)\},$$
$$B_{x,z} = \left\{y \in \mathcal{Y}\colon f_{\tau_{x,z}}(Q_{1-\alpha-\epsilon}(\mu)) < \lambda_{x,y,z} \leq f_{\tau_{x,z}}(\varphi)\right\}.$$

We have

$$\mathbb{P}^{\mathcal{T}}\left(f_{\tau_{x,z}}\left(Q_{1-\alpha}(\mu_n)\right) < \lambda_{x,Y_{n+1},z} \leq f_{\tau_{x,z}}(\varphi) \,|\, X_{n+1}=x, Z_{n+1}=z\right) \leq \mathbb{P}^{\mathcal{T}}\left(A \mid X_{n+1}=x, Z_{n+1}=z\right) + \mathbb{P}^{\mathcal{T}}\left(Y_{n+1} \in B_{x,z} \mid X_{n+1}=x, Z_{n+1}=z\right).$$

Now, let's upper bound the first term of the right-hand side equation. First, remark that

$$\{Q_{1-\alpha}(\mu_n) < Q_{1-\alpha-\epsilon}(\mu)\} \Leftrightarrow \left\{ \frac{1}{n+1} \sum_{k=1}^{n} \mathbb{1}_{f_{\bar{\tau}_k}^{-1}(\bar{\lambda}_k) < Q_{1-\alpha-\epsilon}(\mu)} \geq 1-\alpha \right\}.$$

Thus, we deduce that

$$\mathbb{P}^{\mathcal{T}}\left(A \mid X_{n+1}=x, Z_{n+1}=z\right) \leq \mathbb{P}^{\mathcal{T}}\left(\sum_{k=1}^{n} \mathbb{1}_{f_{\bar{\tau}_k}^{-1}(\bar{\lambda}_k) < Q_{1-\alpha-\epsilon}(\mu)} \geq (n+1)(1-\alpha) \right).$$

Recall that $p_\epsilon = \mathbb{P}^{\mathcal{T}}(f_{\tau_{X,Z}}^{-1}(\lambda_{X,Y,Z}) < Q_{1-\alpha-\epsilon}(\mu))$, and also that we assume $p_\epsilon \leq 1-\alpha$. Therefore, the Bennett's inequality (Boucheron et al., 2003, Theorem 2) implies that

$$\mathbb{P}^{\mathcal{T}}\left(A \mid X_{n+1}=x, Z_{n+1}=z\right) \leq \exp\left(-np_\epsilon(1-p_\epsilon)\, h\left(\frac{(n+1)(1-\alpha) - np_\epsilon}{np_\epsilon(1-p_\epsilon)} \right) \right), \tag{13}$$

where $h : u \mapsto (1+u)\log(1+u) - u$. Moreover, define

$$u_\epsilon = \frac{1-\alpha-p_\epsilon}{p_\epsilon(1-p_\epsilon)}, \qquad \tilde{u}_\epsilon = \frac{(n+1)(1-\alpha) - np_\epsilon}{np_\epsilon(1-p_\epsilon)}.$$

We have $\tilde{u}_\epsilon \leq u_\epsilon$, from the increasing property of h it follows that

$$\mathbb{P}^{\mathcal{T}}\left(A \mid X_{n+1}=x, Z_{n+1}=z\right) \leq \exp\left(-np_\epsilon(1-p_\epsilon)h(u_\epsilon)\right).$$

Furthermore, the definition of $B_{x,z}$ gives

$$\begin{aligned}
&\mathbb{P}^{\mathcal{T}}\left(Y_{n+1} \in B_{x,z} \mid X_{n+1}=x, Z_{n+1}=z\right) \\
&\qquad = \mathbb{P}^{\mathcal{T}}\left(f_{\tau_{x,z}}(Q_{1-\alpha-\epsilon}(\mu)) < \lambda_{x,Y_{n+1},z} \leq f_{\tau_{x,z}}(\varphi) \mid X_{n+1}=x, Z_{n+1}=z \right).
\end{aligned}$$

Moreover, for any $t \in (-\infty, \varphi)$, we have

$$\begin{aligned}
\hat{F}(t) &= \mathbb{P}^{\mathcal{T}}\left(f_{\tau_{X,Z}}^{-1}(\lambda_{X,\hat{Y},Z}) \leq t \right) \\
&= \int \mathbb{P}^{\mathcal{T}}\left(f_{\tau_{X,Z}}^{-1}(\lambda_{X,\hat{Y},Z}) \leq t \,\middle|\, X=x, Z=z \right) \bar{\Pi}_{Z|X=x}(\mathrm{d}z)\, \mathrm{P}_X(\mathrm{d}x) \\
&= \int \mathbb{P}^{\mathcal{T}}\left(\hat{Y} \in \mathcal{R}\left(x, f_{\tau_{z,z}}(t)\right) \,\middle|\, X=x, Z=z \right) \bar{\Pi}_{Z|X=x}(\mathrm{d}z)\, \mathrm{P}_X(\mathrm{d}x).
\end{aligned}$$

Using **H**2, the bijective property of $\tau \mapsto f_\tau(\varphi)$ implies the existence of $\nu \in \mathsf{T}$, such that $f_\nu(\varphi) = f_{\tau_{z,z}}(t)$. Note that, $\nu < \tau_{x,z}$ otherwise it would lead to $f_\nu(\varphi) \geq f_{\tau_{x,z}}(\varphi) > f_{\tau_{x,z}}(t)$. The definition of $\tau_{x,z}$ shows that

$$\mathbb{P}^{\mathcal{T}}\left(\hat{Y} \in \mathcal{R}\left(x, f_\nu(\varphi)\right) \,\middle|\, X=x, Z=z \right) < 1-\alpha.$$

Therefore, we deduce that $Q_{1-\alpha}(\hat{\mu}) \geq \varphi$, and we can conclude that

$$\begin{aligned}
&\mathbb{P}^{\mathcal{T}}\left(Y_{n+1} \in B_{x,z} \mid X_{n+1}=x, Z_{n+1}=z\right) \\
&\qquad \leq \mathbb{P}^{\mathcal{T}}\left(Q_{1-\alpha-\epsilon}(\mu) < f_{\tau_{x,y}}^{-1}(\lambda_{x,Y_{n+1},z}) \leq Q_{1-\alpha}(\hat{\mu}) \mid X_{n+1}=x, Z_{n+1}=z \right).
\end{aligned} \tag{14}$$

Finally, combining (13) and (14) concludes the proof. □

Given $\alpha \in (0,1)$, define the threshold

$$\epsilon_n = \sqrt{\frac{8\alpha(1-\alpha)\log n}{n}}. \tag{15}$$

Lemma A.6. *If the distribution of $f_{\tau_{X,Z}}^{-1}(\lambda_{X,Y,Z})$ is continuous, then for all $\epsilon \in [0, 1-\alpha)$, we have $p_\epsilon = \mathbb{P}^{\mathcal{T}}(f_{\tau_{X,Z}}^{-1}(\lambda_{X,Y,Z}) < Q_{1-\alpha-\epsilon}(\mu)) = 1-\alpha-\epsilon$. Moreover, if $\epsilon_n \leq \frac{\alpha(1-\alpha)}{8}$, then it follows*

$$\exp\left(-np_{\epsilon_n}(1-p_{\epsilon_n}) h\left(\frac{1-\alpha-p_{\epsilon_n}}{p_{\epsilon_n}(1-p_{\epsilon_n})} \right) \right) \leq \frac{1}{n},$$

where $h : u \mapsto (1+u)\log(1+u) - u$.

Proof. First, recall that $Q_{1-\alpha-\epsilon}(\mu)$ is defined in (12). If the distribution of $f^{-1}_{\tau_{X,Z}}(\lambda_{X,Y,Z})$ is continuous, then we have

$$1-\alpha-\epsilon \leq F(Q_{1-\alpha-\epsilon}(\mu)) = \sup_{\delta>0} F(Q_{1-\alpha-\epsilon}(\mu)-\delta)$$
$$\leq \mathbb{P}^{\mathcal{T}}\left(f^{-1}_{\tau_{X,Z}}(\lambda_{X,Y,Z}) < Q_{1-\alpha-\epsilon}(\mu)\right) = p_\epsilon \leq 1-\alpha-\epsilon.$$

Therefore, we deduce that $p_\epsilon = 1-\alpha-\epsilon$. Let's denote

$$\delta_n = (n+1)(1-\alpha) - np_{\epsilon_n}, \qquad u_n = \frac{(n+1)(1-\alpha)-np_{\epsilon_n}}{np_{\epsilon_n}(1-p_{\epsilon_n})}.$$

For any $u \geq 0$, remark that $\log(1+u) \geq u - u^2/2$. Thus, we deduce

$$np_{\epsilon_n}(1-p_{\epsilon_n})\, h\,(u_n) \geq \delta_n \frac{(1+u_n)\log(1+u_n)-u_n}{u_n}$$
$$\geq \delta_n \frac{u_n(1-u_n)}{2}. \tag{16}$$

Now, let's show that $u_n \leq 1/4$. We have

$$u_n = \frac{(n+1)(1-\alpha)-np_{\epsilon_n}}{np_{\epsilon_n}(1-p_{\epsilon_n})}$$
$$= \frac{1-\alpha}{np_{\epsilon_n}(1-p_{\epsilon_n})} + \frac{1-\alpha-p_{\epsilon_n}}{p_{\epsilon_n}(1-p_{\epsilon_n})}$$
$$= \frac{1-\alpha}{n(\alpha+\epsilon_n)(1-\alpha-\epsilon_n)} + \frac{\epsilon_n}{(\alpha+\epsilon_n)(1-\alpha-\epsilon_n)}.$$

Therefore, $u_n \leq 1/4$ if and only if

$$\frac{1-\alpha}{n} + \epsilon_n \leq \frac{(\alpha+\epsilon_n)(1-\alpha-\epsilon_n)}{4}.$$

The function $\epsilon \in [0, 1/2-\alpha] \mapsto (\alpha+\epsilon)(1-\alpha-\epsilon)$ is increasing. Since $\epsilon_n \leq \alpha(1-\alpha)/8 \leq 1/2-\alpha$, it is sufficient to prove that

$$\frac{1-\alpha}{n} + \epsilon_n \leq \frac{\alpha(1-\alpha)}{4}.$$

Since $\epsilon_n \leq \alpha(1-\alpha)/8$, we just need to show that

$$\frac{1-\alpha}{n} \leq \frac{\alpha(1-\alpha)}{8}, \qquad \text{i.e.,} \qquad \frac{8\alpha(1-\alpha)}{n} \leq \alpha^2(1-\alpha). \tag{17}$$

Again, using the fact that $\epsilon_n \leq \alpha(1-\alpha)/8$, we deduce that

$$\frac{8\alpha(1-\alpha)}{n} = \frac{\epsilon_n^2}{\log n} \leq \frac{\alpha^2(1-\alpha)^2}{8\log n} = \alpha^2(1-\alpha) \times \frac{(1-\alpha)}{8\log n}.$$

Since $\frac{(1-\alpha)}{8\log n} \leq 1$, we deduce that (17) holds. This concludes that $u_n \leq 1/4$. Moreover, for any $u \in [0, 0.25]$, we have

$$\delta_n \frac{u(1-u)}{2} \geq \frac{u\delta_n}{4}.$$

Plugging the previous line in (16) implies that

$$\exp\left(-np_{\epsilon_n}(1-p_{\epsilon_n})\, h\,(u_n)\right) \leq \exp\left(-\frac{[(n+1)(1-\alpha)-np_{\epsilon_n}]^2}{4np_{\epsilon_n}(1-p_{\epsilon_n})}\right)$$
$$\leq \exp\left(-\frac{(1-\alpha+n\epsilon_n)^2}{4n(\alpha+\epsilon_n)(1-\alpha-\epsilon_n)}\right)$$
$$\leq \exp\left(-\frac{n\epsilon_n^2}{4(\alpha+\epsilon_n)(1-\alpha-\epsilon_n)}\right). \tag{18}$$

Lastly, since $\epsilon_n \leq \alpha$, it follows that

$$\frac{n\epsilon_n^2}{4(\alpha+\epsilon_n)(1-\alpha-\epsilon_n)} = \frac{2\alpha(1-\alpha)\log n}{(\alpha+\epsilon_n)(1-\alpha-\epsilon_n)} \geq \log n.$$

Combining the previous line with (18) completes the proof. □

For any $\epsilon \in [0, \alpha)$, define

$$q_\epsilon = \mathbb{P}^{\mathcal{T}}(f^{-1}_{\tau_{X,Z}}(\lambda_{X,Y,Z}) < Q_{1-\alpha+\epsilon}(\mu)).$$

Theorem A.7. *Assume **H**1-**H**2 hold, and let $x \in \mathbb{R}^d$ be such that $\Pi_{Y|X=x}$ is a probability measure. If the distribution of $f^{-1}_{\tau_{X,Z}}(\lambda_{X,Y,Z})$ is continuous and $n^{-1}\log n \leq 8^{-3}\alpha(1-\alpha)$, then, it holds*

$$q^{(x,z)}_{n+1} \leq \frac{1}{n} + \mathbb{P}^{\mathcal{T}}\left(Q_{1-\alpha}(\hat{\mu}) < f^{-1}_{\tau_{x,y}}(\lambda_{x,Y_{n+1},z}) \leq Q_{1-\alpha+\epsilon_n}(\mu) \,|\, X_{n+1} = x, Z_{n+1} = z\right), \quad (19)$$

where ϵ_n is defined in (15).

Proof. Let's consider

$$A = \{Q_{1-\alpha+\epsilon_n}(\mu) < Q_{1-\alpha}(\mu_n)\},$$
$$B_{x,z} = \left\{y \in \mathcal{Y} \colon f_{\tau_{x,z}}(Q_{1-\alpha}(\hat{\mu})) < \lambda_{x,y,z} \leq f_{\tau_{x,z}}(Q_{1-\alpha+\epsilon_n}(\mu))\right\}.$$

We have

$$\begin{aligned}\mathbb{P}^{\mathcal{T}}&\left(f_{\tau_{x,z}}(Q_{1-\alpha}(\hat{\mu})) < \lambda_{x,Y_{n+1},z} \leq f_{\tau_{x,z}}(Q_{1-\alpha}(\mu_n)) \,|\, X_{n+1} = x, Z_{n+1} = z\right) \\ &\leq \mathbb{P}^{\mathcal{T}}(A \mid X_{n+1} = x, Z_{n+1} = z) + \mathbb{P}^{\mathcal{T}}(Y_{n+1} \in B_{x,z} \mid X_{n+1} = x, Z_{n+1} = z). \quad (20)\end{aligned}$$

Now, let's upper bound the first term of the right-hand side equation. First, remark that

$$\{Q_{1-\alpha+\epsilon_n}(\mu) < Q_{1-\alpha}(\mu_n)\} \Leftrightarrow \left\{\frac{1}{n+1}\sum_{k=1}^{n} \mathbb{1}_{f^{-1}_{\bar{\tau}_k}(\bar{\lambda}_k) < Q_{1-\alpha+\epsilon_n}(\mu)} < 1-\alpha\right\}.$$

Thus, we deduce that

$$\mathbb{P}^{\mathcal{T}}(A \mid X_{n+1} = x, Z_{n+1} = z) \leq \mathbb{P}^{\mathcal{T}}\left(\sum_{k=1}^{n} \mathbb{1}_{f^{-1}_{\bar{\tau}_k}(\bar{\lambda}_k) < Q_{1-\alpha+\epsilon_n}(\mu_n)} < (n+1)(1-\alpha)\right).$$

Recall that $q_{\epsilon_n} = \mathbb{P}^{\mathcal{T}}(f^{-1}_{\tau_{X,Z}}(\lambda_{X,Y,Z}) < Q_{1-\alpha+\epsilon_n}(\mu))$, and also that $q_{\epsilon_n} < 1$ since the distribution of $f^{-1}_{\tau_{X,Z}}(\lambda_{X,Y,Z})$ is continuous with $1-\alpha+\epsilon_n < 1$. Therefore, the Bennett's inequality (Boucheron et al., 2003, Theorem 2) implies that

$$\mathbb{P}^{\mathcal{T}}(A \mid X_{n+1} = x, Z_{n+1} = z) \leq \exp\left(-nq_{\epsilon_n}(1-q_{\epsilon_n})\, h\left(\frac{(n+1)(1-\alpha) - nq_{\epsilon_n}}{nq_{\epsilon_n}(1-q_{\epsilon_n})}\right)\right),$$

where $h : u \mapsto (1+u)\log(1+u) - u$. Moreover, define

$$u_{\epsilon_n} = \frac{1-\alpha-q_{\epsilon_n}}{q_{\epsilon_n}(1-q_{\epsilon_n})}, \qquad \tilde{u}_{\epsilon_n} = \frac{(n+1)(1-\alpha) - nq_{\epsilon_n}}{nq_{\epsilon_n}(1-q_{\epsilon_n})}.$$

We have $\tilde{u}_{\epsilon_n} \leq u_{\epsilon_n}$, from the increasing property of h combined with Lemma A.6, it follows that

$$\mathbb{P}^{\mathcal{T}}(A \mid X_{n+1} = x, Z_{n+1} = z) \leq \exp\left(-nq_{\epsilon_n}(1-q_{\epsilon_n})h(u_{\epsilon_n})\right) \leq n^{-1}.$$

The previous inequality combined with (20) concludes the proof. □

A.3 Proof of Theorem 3.3

Theorem A.8. *Assume **H**1-**H**2 and suppose the distributions of $f^{-1}_{\tau_{X,Z}}(\lambda_{X,Y,Z})$ and $f^{-1}_{\tau_{X,Z}}(\lambda_{X,\hat{Y},Z})$ are continuous. For any $\alpha \in (0,1)$ and $\rho > 0$, it holds*

$$\begin{aligned}\mathbb{P}^{\mathcal{T}}&\left(\left|\mathbb{P}^{\mathcal{T}}(Y_{n+1} \in \mathcal{C}_\alpha(X_{n+1}) \,|\, X_{n+1}, Z_{n+1}) - 1 + \alpha\right| > \rho\right) \\ &\leq \frac{2n^{-1} + \sqrt{128\alpha(1-\alpha)n^{-1}\log n} + 4\mathrm{d_{TV}}(\mathrm{P}_{X,Y}; \mathrm{P}_X \times \Pi_{Y|X})}{\rho}.\end{aligned}$$

Proof. Let $\rho > 0$ be fixed. Applying Theorem 3.2, we obtain that

$$\begin{aligned}1-\alpha-\mathrm{d_{TV}}(\mathrm{P}_{Y|X=x}; \Pi_{Y|X=x}) - p^{(x,z)}_{n+1} &\leq \mathbb{P}^{\mathcal{T}}(Y_{n+1} \in \mathcal{C}_\alpha(X_{n+1}) \mid X_{n+1} = x, Z_{n+1} = z) \\ &\leq \Pi_{Y|X=x}(\mathcal{R}_z(x; f_{\tau_{x,z}}(\varphi))) + \mathrm{d_{TV}}(\mathrm{P}_{Y|X=x}; \Pi_{Y|X=x}) + q^{(x,z)}_{n+1}. \quad (21)\end{aligned}$$

Step 1: Lower bound. Using the Markov's inequality implies that

$$\mathbb{P}^{\mathcal{T}}\left(\mathbb{P}^{\mathcal{T}}\left(Y_{n+1}\in\mathcal{C}_\alpha(X_{n+1})\,|\,X_{n+1},Z_{n+1}\right)<1-\alpha-\rho\right)\leq\mathbb{P}^{\mathcal{T}}\left(\mathrm{d_{TV}}(\mathrm{P}_{Y|X};\Pi_{Y|X})+p_{n+1}^{(X,Z)}<\rho\right)$$
$$\leq\frac{\mathbb{E}^{\mathcal{T}}\left[\mathrm{d_{TV}}(\mathrm{P}_{Y|X};\Pi_{Y|X})\right]+\mathbb{E}^{\mathcal{T}}\left[p_{n+1}^{(X,Z)}\right]}{\rho}. \quad (22)$$

Moreover, using Theorem A.5 with $\Phi(\epsilon)=\epsilon[(u_\epsilon^{-1}-1)\log(1+u_\epsilon)-1]$ and $u_\epsilon=\epsilon(\alpha+\epsilon)^{-1}(1-\alpha-\epsilon)$, it holds

$$\mathbb{E}^{\mathcal{T}}\left[p_{n+1}^{(X,Z)}\right]=\mathbb{P}^{\mathcal{T}}\left(Q_{1-\alpha}(\mu_n)<f^{-1}_{\tau_{X,Z}}(\lambda_{X,Y,Z})\leq\varphi\right)$$
$$\leq\exp\left(-n\Phi(\epsilon)\right)+\mathbb{P}^{\mathcal{T}}\left(Q_{1-\alpha-\epsilon}(\mu)<f^{-1}_{\bar{\tau}_{n+1}}(\bar{\lambda}_{n+1})\leq Q_{1-\alpha}(\hat{\mu})\,\middle|\,X_{n+1}=x,Z_{n+1}=z\right).$$

By Lemma A.6, if $n^{-1}\log n\leq 8^{-3}\alpha(1-\alpha)$, then, setting $\epsilon_n=\sqrt{8\alpha(1-\alpha)n^{-1}\log n}$ ensures that $\exp(-n\Phi(\epsilon_n))\leq n^{-1}$. We assume in the following that $n^{-1}\log n\leq 8^{-3}\alpha(1-\alpha)$, because, if it not the case, the final upper bound obtained at the end of the proof is still valid. Thus, we get

$$\mathbb{E}^{\mathcal{T}}\left[p_{n+1}^{(X,Z)}\right]\leq n^{-1}+\mathbb{P}^{\mathcal{T}}\left(Q_{1-\alpha-\epsilon_n}(\mu)<f^{-1}_{\bar{\tau}_{n+1}}(\bar{\lambda}_{n+1})\leq Q_{1-\alpha}(\hat{\mu})\right). \quad (23)$$

Let's define $\bar{\gamma}$ by

$$\bar{\gamma}=\min(1,1-\alpha+\mathrm{d_{TV}}(\mathrm{P}_{X,Y};\mathrm{P}_X\times\Pi_{Y|X})).$$

We now show that $Q_{1-\alpha}(\hat{\mu})\leq Q_{\bar{\gamma}}(\mu)$. By continuity of the cumulative density function of $f^{-1}_{\tau_{X,Z}}(\lambda_{X,\hat{Y},Z})$, we have

$$1-\alpha=\mathbb{P}^{\mathcal{T}}\left(f^{-1}_{\tau_{X,Z}}(\lambda_{X,\hat{Y},Z})\leq Q_{1-\alpha}(\hat{\mu})\right)$$
$$\geq\mathbb{P}^{\mathcal{T}}\left(f^{-1}_{\tau_{X,Z}}(\lambda_{X,Y,Z})\leq Q_{1-\alpha}(\hat{\mu})\right)-\mathrm{d_{TV}}(\mathrm{P}_{X,Y};\mathrm{P}_X\times\Pi_{Y|X}).$$

Hence, it follows that

$$\mathbb{P}^{\mathcal{T}}\left(f^{-1}_{\tau_{X,Z}}(\lambda_{X,Y,Z})\leq Q_{1-\alpha}(\hat{\mu})\right)\leq\bar{\gamma}\leq\mathbb{P}^{\mathcal{T}}\left(f^{-1}_{\tau_{X,Z}}(\lambda_{X,Y,Z})\leq Q_{\bar{\gamma}}(\mu)\right).$$

Thus, the previous line implies that $Q_{1-\alpha}(\hat{\mu})\leq Q_{\bar{\gamma}}(\mu)$. Once again, using the continuity of the distribution of $f^{-1}_{\tau_{X,Z}}(\lambda_{X,Y,Z})$, we can write

$$\mathbb{P}^{\mathcal{T}}\left(Q_{1-\alpha}(\hat{\mu})<f^{-1}_{\tau_{x,y}}(\lambda_{x,Y_{n+1},z})\leq Q_{1-\alpha+\epsilon_n}(\mu)\right)\leq\mathbb{P}^{\mathcal{T}}\left(Q_{1-\alpha-\epsilon_n}(\mu)<f^{-1}_{\bar{\tau}_{n+1}}(\bar{\lambda}_{n+1})\leq Q_{\bar{\gamma}}(\mu)\right)$$
$$=F\left(Q_{\bar{\gamma}}(\mu)\right)-F\left(Q_{1-\alpha-\epsilon_n}(\mu)\right)=\bar{\gamma}+\epsilon_n-1+\alpha$$
$$=n^{-1}+\sqrt{8\alpha(1-\alpha)n^{-1}\log n}+\mathrm{d_{TV}}(\mathrm{P}_{X,Y};\mathrm{P}_X\times\Pi_{Y|X}).$$

Plugging the previous inequality inside (23) yields

$$\mathbb{E}^{\mathcal{T}}\left[p_{n+1}^{(X,Z)}\right]\leq n^{-1}+\sqrt{8\alpha(1-\alpha)n^{-1}\log n}+\mathrm{d_{TV}}(\mathrm{P}_{X,Y};\mathrm{P}_X\times\Pi_{Y|X}).$$

Therefore, (22) implies that

$$\mathbb{P}^{\mathcal{T}}\left(\mathbb{P}^{\mathcal{T}}\left(Y_{n+1}\in\mathcal{C}_\alpha(X_{n+1})\,|\,X_{n+1},Z_{n+1}\right)<1-\alpha-\rho\right)$$
$$\leq\frac{n^{-1}+\sqrt{8\alpha(1-\alpha)n^{-1}\log n}+\mathrm{d_{TV}}(\mathrm{P}_{X,Y};\mathrm{P}_X\times\Pi_{Y|X})+\mathbb{E}^{\mathcal{T}}\left[\mathrm{d_{TV}}(\mathrm{P}_{Y|X};\Pi_{Y|X})\right]}{\rho}. \quad (24)$$

Step 2: Upper bound. Using (21), we obtain

$$\mathbb{P}^{\mathcal{T}}\left(\mathbb{P}^{\mathcal{T}}\left(Y_{n+1}\in\mathcal{C}_\alpha(X_{n+1})\,|\,X_{n+1},Z_{n+1}\right)>1-\alpha+\rho\right)$$
$$\leq\mathbb{P}^{\mathcal{T}}\left(\Pi_{Y|X=X}(\mathcal{R}_Z(X;f_{\tau_{X,Z}}(\varphi)))+\mathrm{d_{TV}}(\mathrm{P}_{Y|X=X};\Pi_{Y|X=X})+q_{n+1}^{(X,Z)}>1-\alpha+\rho\right).$$

The continuity of the distribution of $f^{-1}_{\tau_{X,Z}}(\lambda_{X,\hat{Y},Z})$ implies

$$1-\alpha=\mathbb{P}^{\mathcal{T}}\left(f^{-1}_{\tau_{X,Z}}(\lambda_{X,\hat{Y},Z})\leq\varphi\right)=\int\Pi_{Y|X=x}(\mathcal{R}_z(x;f_{\tau_{x,z}}(\varphi)))\bar{\Pi}_{Z|X=x}(\mathrm{d}z)\mathrm{P}_X(\mathrm{d}x).$$

Since $\Pi_{Y|X=x}(\mathcal{R}_z(x; f_{\tau_{x,z}}(\varphi))) \geq 1-\alpha$, we deduce that $\Pi_{Y|X=x}(\mathcal{R}_z(x; f_{\tau_{x,z}}(\varphi))) = 1-\alpha$ almost surely. Therefore, using the Markov's inequality gives

$$\mathbb{P}^{\mathcal{T}}\left(\mathbb{P}^{\mathcal{T}}\left(Y_{n+1} \in \mathcal{C}_\alpha(X_{n+1}) \,|\, X_{n+1}, Z_{n+1}\right) > 1-\alpha+\rho\right) \leq \frac{\mathbb{E}^{\mathcal{T}}\left[\mathrm{d_{TV}}(\mathrm{P}_{Y|X}; \Pi_{Y|X})\right] + \mathbb{E}^{\mathcal{T}}\left[q_{n+1}^{(X,Z)}\right]}{\rho}. \tag{25}$$

Moreover, applying Theorem A.7 shows that

$$q_{n+1}^{(x,z)} \leq n^{-1} + \mathbb{P}^{\mathcal{T}}\left(Q_{1-\alpha}(\hat{\mu}) < f^{-1}_{\tau_{x,y}}(\lambda_{x,Y_{n+1},z}) \leq Q_{1-\alpha+\epsilon_n}(\mu) \,|\, X_{n+1}=x, Z_{n+1}=z\right). \tag{26}$$

Let's define $\underline{\gamma}$ by

$$\underline{\gamma} = \min(1, 1-\alpha-\mathrm{d_{TV}}(\mathrm{P}_{X,Y}; \mathrm{P}_X \times \Pi_{Y|X})).$$

We now show that $Q_{\underline{\gamma}}(\mu) \leq Q_{1-\alpha}(\hat{\mu})$. By continuity of the cumulative density function of $f^{-1}_{\tau_{X,Z}}(\lambda_{X,\hat{Y},Z})$, we have

$$\begin{aligned}
1-\alpha &= \mathbb{P}^{\mathcal{T}}\left(f^{-1}_{\tau_{X,Z}}(\lambda_{X,\hat{Y},Z}) \leq Q_{1-\alpha}(\hat{\mu})\right) \\
&\leq \mathbb{P}^{\mathcal{T}}\left(f^{-1}_{\tau_{X,Z}}(\lambda_{X,Y,Z}) \leq Q_{1-\alpha}(\hat{\mu})\right) + \mathrm{d_{TV}}(\mathrm{P}_{X,Y}; \mathrm{P}_X \times \Pi_{Y|X}).
\end{aligned}$$

Hence, it follows that

$$\underline{\gamma} \leq \mathbb{P}^{\mathcal{T}}\left(f^{-1}_{\tau_{X,Z}}(\lambda_{X,Y,Z}) \leq Q_{1-\alpha}(\hat{\mu})\right).$$

Thus, we deduce that $Q_{1-\alpha}(\hat{\mu}) \geq Q_{\underline{\gamma}}(\mu)$. Using the continuity of the distribution of $f^{-1}_{\tau_{X,Z}}(\lambda_{X,Y,Z})$, we can write

$$\begin{aligned}
\mathbb{P}^{\mathcal{T}}\left(Q_{1-\alpha}(\hat{\mu}) < f^{-1}_{\tau_{x,y}}(\lambda_{x,Y_{n+1},z}) \leq Q_{1-\alpha+\epsilon_n}(\mu)\right) &\leq \mathbb{P}^{\mathcal{T}}\left(Q_{\underline{\gamma}}(\mu) < f^{-1}_{\tau_{x,y}}(\lambda_{x,Y_{n+1},z}) \leq Q_{1-\alpha+\epsilon_n}(\mu)\right) \\
&= F\left(Q_{1-\alpha+\epsilon_n}(\mu)\right) - F\left(Q_{\underline{\gamma}}(\mu)\right) = \epsilon_n - 1 + \alpha - \underline{\gamma} \\
&= n^{-1} + \sqrt{8\alpha(1-\alpha)n^{-1}\log n} + \mathrm{d_{TV}}(\mathrm{P}_{X,Y}; \mathrm{P}_X \times \Pi_{Y|X}).
\end{aligned}$$

Plugging the previous inequality inside (26) yields

$$\mathbb{E}^{\mathcal{T}}\left[q_{n+1}^{(X,Z)}\right] \leq n^{-1} + \sqrt{8\alpha(1-\alpha)n^{-1}\log n} + \mathrm{d_{TV}}(\mathrm{P}_{X,Y}; \mathrm{P}_X \times \Pi_{Y|X}).$$

Therefore, (25) implies that

$$\begin{aligned}
&\mathbb{P}^{\mathcal{T}}\left(\mathbb{P}^{\mathcal{T}}\left(Y_{n+1} \in \mathcal{C}_\alpha(X_{n+1}) \,|\, X_{n+1}, Z_{n+1}\right) < 1-\alpha-\rho\right) \\
&\leq \frac{n^{-1} + \sqrt{8\alpha(1-\alpha)n^{-1}\log n} + \mathrm{d_{TV}}(\mathrm{P}_{X,Y}; \mathrm{P}_X \times \Pi_{Y|X}) + \mathbb{E}^{\mathcal{T}}\left[\mathrm{d_{TV}}(\mathrm{P}_{Y|X}; \Pi_{Y|X})\right]}{\rho}.
\end{aligned} \tag{27}$$

Step 3: Bound on $\mathbb{E}^{\mathcal{T}}\left[\mathrm{d_{TV}}(\mathbf{P}_{Y|X}; \Pi_{Y|X})\right]$. Let's denote $\nu_{Y|X=x} = 2^{-1}(\mathrm{P}_{Y|X=x} + \Pi_{Y|X=x})$. Since $\mathrm{P}_{Y|X=x} \ll \nu_{Y|X=x}$ and $\Pi_{Y|X=x} \ll \nu_{Y|X=x}$, there exists two Radon–Nikodym derivatives $g_1(x,\cdot)$ and $g_1(x,\cdot)$ of $\mathrm{P}_{Y|X=x}$ and $\Pi_{Y|X=x}$ with respect to $\nu_{Y|X=x}$. Moreover, g_1 and g_2 are also the Radon–Nikodym derivatives of $\mathrm{P}_{X,Y}$ and $\mathrm{P}_X \times \Pi_{Y|X}$ with respect to $\mathrm{P}_X \times \nu_{Y|X}$. By definition of the total variation distance, we have

$$\begin{aligned}
\mathbb{E}^{\mathcal{T}}\left[\mathrm{d_{TV}}(\mathrm{P}_{Y|X}; \Pi_{Y|X})\right] &= \int \mathrm{d_{TV}}(\mathrm{P}_{Y|X}; \Pi_{Y|X}) \mathrm{P}_X(\mathrm{d}x) \\
&= \frac{1}{2}\int |g_1(x,y) - g_2(x,y)| \, \nu_{Y|X=x} \mathrm{P}_X(\mathrm{d}x) \\
&= \mathrm{d_{TV}}(\mathrm{P}_{X,Y}; \mathrm{P}_X \times \Pi_{Y|X}).
\end{aligned} \tag{28}$$

Step 4: Combination. Finally, using (24)-(27) and (28), it follows that

$$\mathbb{P}^{\mathcal{T}}\left(\left|\mathbb{P}^{\mathcal{T}}\left(Y_{n+1}\in\mathcal{C}_\alpha(X_{n+1})\,|\,X_{n+1},Z_{n+1}\right)-1+\alpha\right|>\rho\right) \leq \frac{2n^{-1}+\sqrt{128\alpha(1-\alpha)n^{-1}\log n}+4\mathrm{d_{TV}}(\mathrm{P}_{X,Y};\mathrm{P}_X\times\Pi_{Y|X})}{\rho}.$$

Note that the proof assumes $n^{-1}\log n \leq 8^{-3}\alpha(1-\alpha)$. To ensure the validity of the previous bound even when this assumption does not hold, we increased the term $\sqrt{32\alpha(1-\alpha)n^{-1}\log n}$ to $\sqrt{128\alpha(1-\alpha)n^{-1}\log n}$. □

Theorem A.9. *Assume **H1**-**H2**-**H3** hold. If the distributions of $f^{-1}_{\tau_{X,Z}}(\lambda_{X,Y,Z})$ and $f^{-1}_{\tau_{X,Z}}(\lambda_{X,\hat{Y},Z})$ are continuous, then, $\forall\epsilon\in(0,1)$ there exists $(\Lambda_n^{(\epsilon)})_{n\in\mathbb{N}}$ such that $\liminf_{n\to\infty}\mathbb{P}((X_{n+1},Z_{n+1})\in\Lambda_n^{(\epsilon)})\geq 1-\epsilon$ and also*

$$\sup_{(x,z)\in\Lambda_n^{(\epsilon)}}\left|\mathbb{P}^{\mathcal{T}}\left(Y_{n+1}\in\mathcal{C}_\alpha(X_{n+1})\,|\,(X_{n+1},Z_{n+1})=(x,z)\right)-1+\alpha\right|=\mathrm{O}_{\mathbb{P}}\left(\sqrt{n^{-1}\log n}+r_n\right).$$

Proof. First of all, define the following variables

$$c_{n+1}(x,z)=\left|\mathbb{P}^{\mathcal{T}}\left(Y_{n+1}\in\mathcal{C}_\alpha(X_{n+1})\,|\,(X_{n+1},Z_{n+1})=(x,z)\right)-1+\alpha\right|,$$
$$d_n=\mathrm{d_{TV}}(\mathrm{P}_{X,Y};\mathrm{P}_X\times\Pi^{(m_n)}_{Y|X}).$$

Applying Theorem A.8, we obtain

$$\begin{aligned}\mathbb{P}\left(c_{n+1}(X_{n+1},Z_{n+1})>\rho\right)&\leq\mathbb{P}\left(d_n>r_n\right)+\mathbb{P}\left(c_{n+1}(X_{n+1},Z_{n+1})>\rho;d_n\leq r_n\right)\\&\leq\mathbb{P}\left(d_n>r_n\right)+\mathbb{E}\left[\mathbb{1}_{d_n\leq r_n}\mathbb{P}^{\mathcal{T}}\left(c_{n+1}(X_{n+1},Z_{n+1})>\rho\right)\right]\\&\leq\mathbb{P}\left(d_n>r_n\right)+\frac{2n^{-1}+\sqrt{128\alpha(1-\alpha)n^{-1}\log n}+4r_n}{\rho}.\end{aligned}$$

Finally, using **H3**, we get $\lim_{n\to\infty}\mathbb{P}(d_n>r_n)=0$. Therefore, for any $\epsilon>0$, there exist $M_\epsilon>0$ and $\tilde{n}_\epsilon\in\mathbb{N}$ such that, $\forall n\geq\tilde{n}_\epsilon$, it holds

$$\mathbb{P}\left(c_{n+1}(X_{n+1},Z_{n+1})>M_\epsilon\times\left(\sqrt{n^{-1}\log n}+r_n\right)\right)\leq\epsilon. \tag{29}$$

Given $\epsilon\in(0,1)$, let's consider the following set

$$\Lambda_n^{(\epsilon)}=\left\{(X_{n+1}(\omega),Z_{n+1}(\omega))\colon\omega\in\Omega,c_{n+1}(X_{n+1},Z_{n+1})(\omega)\leq M_\epsilon\times\left(\sqrt{n^{-1}\log n}+r_n\right)\right\}.$$

Equation (29) implies that

$$\liminf_{n\to\infty}\mathbb{P}\left((X_{n+1},Z_{n+1})\in\Lambda_n^{(\epsilon)}\right)\geq 1-\epsilon,$$

and by definition of $\Lambda_n^{(\epsilon)}$, we also have

$$\sup_{(x,z)\in\Lambda_n^{(\epsilon)}}c_{n+1}(x,z)=\mathrm{O}_{\mathbb{P}}\left(\sqrt{n^{-1}\log n}+r_n\right).$$

□

Note that, (29) also shows that

$$\left|\mathbb{P}^{\mathcal{T}}\left(Y_{n+1}\in\mathcal{C}_\alpha(X_{n+1})\,|\,X_{n+1},Z_{n+1}\right)-1+\alpha\right|=\mathrm{O}_{\mathbb{P}}\left(n^{-1/2}\sqrt{\log n}+r_n\right).$$

A.4 ADDITIONAL RESULTS

Let's denote the conditional c.d.f of $f^{-1}_{\tau_{X,Z}}(\lambda_{X,Y,Z})$ by

$$F_{x,z}(\cdot) = \int_{\mathbb{R}^d \times \mathcal{Z}} \mathbb{P}\left(f^{-1}_{\tau_{x,z}}(\lambda_{x,Y,z}) \leq \cdot \mid (X,Z) = (x,z)\right) \bar{\Pi}_{Z|X=x}(\mathrm{d}z)\mathrm{P}_X(\mathrm{d}x).$$

Lemma A.10. *Assume that $Q_{1-\alpha}(\mu_n) \to \varphi$ almost-surely as $n \to \infty$. If $F_{X,Z}$ is continuous almost-surely, then $\lim_{n\to\infty} p^{(x,z)}_{n+1} = 0$, $\bar{\Pi}_{Z|X} \times \mathrm{P}_X$-almost everywhere.*

Proof. First, define the following sets:

$$A = \left\{\omega \in \Omega \colon \lim_{n\to\infty} Q_{1-\alpha}(\mu_n(\omega)) = \varphi\right\},$$
$$B = \left\{\omega \in \Omega \colon F_{X(\omega),Z(\omega)} \text{ is continuous}\right\}.$$

For all $\omega \in A \cap B$, it holds

$$\lim_{n\to\infty} F_{X(\omega),Z(\omega)}\left(Q_{1-\alpha}\left(\mu_n(\omega)\right) \wedge \varphi\right) = F_{X(\omega),Z(\omega)}\left(\varphi\right).$$

Moreover, note that we can write

$$p^{(x,z)}_{n+1} = F_{x,z}(\varphi) - F_{x,z}(\varphi \wedge Q_{1-\alpha}(\mu_n)).$$

Hence, we deduce that

$$\begin{aligned}
1 = \mathbb{P}\left(A \cap B\right) &\leq \mathbb{P}\left(\omega \in \Omega \colon \lim_{n\to\infty} F_{X(\omega),Z(\omega)}\left(Q_{1-\alpha}\left(\mu_n(\omega)\right) \wedge \varphi\right) = F_{X(\omega),Z(\omega)}\left(\varphi\right)\right) \\
&= \mathbb{P}\left(\lim_{n\to\infty} p^{(X,Z)}_{n+1} = 0\right) \\
&= \int_{\mathbb{R}^d \times \mathcal{Z}} \mathbb{P}\left(\lim_{n\to\infty} p^{(x,z)}_{n+1} = 0 \,\middle|\, (X,Z) = (x,z)\right) \mathrm{P}_{Z|X=x}(\mathrm{d}z)\, \mathrm{P}_X(\mathrm{d}x).
\end{aligned}$$

The last line implies that $p^{(x,z)}_{n+1} \to 0$ almost $\mathrm{P}_{Z|X} \times \mathrm{P}_X$-everywhere. □

The prediction set, defined in (4), is derived from the $(1-\alpha)$-quantile of the conformity scores $\{f^{-1}_{\bar{\tau}_k}(\bar{\lambda}_k)\}_{k=1}^n \cup \{\infty\}$. However, $\{\infty\}$ can be removed from these conformity scores. Inspired by Romano et al. (2019); Sesia & Candès (2020), we prove a corollary of Theorem 3.1. Its result demonstrates the marginal validity of the prediction set defined as

$$\bar{\mathcal{C}}_\alpha(x) = \mathcal{R}_z\left(x; f_{\tau_{x,z}}\left(Q_{(1-\alpha)(1+n^{-1})}\left(\tfrac{1}{n}\textstyle\sum_{k=1}^n \delta_{f^{-1}_{\bar{\tau}_k}(\bar{\lambda}_k)}\right)\right)\right). \tag{30}$$

While the prediction set $\bar{\mathcal{C}}_\alpha(x)$ relies on the quantile of the distribution $\frac{1}{n}\sum_{k=1}^n \delta_{f^{-1}_{\bar{\tau}_k}(\bar{\lambda}_k)}$, its proof reveals that this prediction set is equivalent to $\mathcal{C}_\alpha(x)$.

Corollary A.11. *Under the same assumptions as in Theorem 3.1, for any $\alpha \in [1/(n+1), 1]$, we have*

$$1 - \alpha \leq \mathbb{P}\left(Y_{n+1} \in \bar{\mathcal{C}}_\alpha(X_{n+1})\right) < 1 - \alpha + \frac{1}{n+1},$$

where the upper bound only holds if the conformity scores $\{f^{-1}_{\bar{\tau}_k}(\bar{\lambda}_k)\}_{k=1}^{n+1}$ are almost surely distinct.

Proof. Let $\alpha \in \mathbb{R}$ such that $(n+1)^{-1} \leq \alpha \leq 1$, and recall that

$$\mu_n = \frac{1}{n+1}\sum_{k=1}^n \delta_{f^{-1}_{\bar{\tau}_k}(\bar{\lambda}_k)} + \frac{1}{n+1}\delta_\infty.$$

Since $\alpha \geq (n+1)^{-1}$, the quantile $Q_{1-\alpha}(\mu_n)$ is the k_αth order statistic of $V_1, \ldots, V_n$, where

$$V_k = f^{-1}_{\bar{\tau}_k}(\bar{\lambda}_k), \quad \text{and} \quad k_\alpha = \lceil (1-\alpha)(n+1) \rceil.$$

However, $\forall \beta \in (\frac{k_\alpha - 1}{n}, \frac{k_\alpha}{n}]$, we have

$$Q_\beta\left(\frac{1}{n}\sum_{k=1}^{n}\delta_{V_k}\right) = V_{(k_\alpha)}.$$

Since $\mathcal{C}_\alpha(X_{n+1}) = \mathcal{R}_{Z_{n+1}}(X_{n+1}; f_{\bar{\tau}_{n+1}}(V_{(k_\alpha)}))$, Theorem 3.1 implies that

$$1-\alpha \leq \mathbb{P}\left(Y_{n+1} \in \mathcal{R}_{Z_{n+1}}\left(X_{n+1}; f_{\bar{\tau}_{n+1}}\left(Q_\beta\left(\frac{1}{n}\sum_{k=1}^{n}\delta_{V_k}\right)\right)\right)\right) < 1-\alpha+\frac{1}{n+1}.$$

Setting $\beta = (1-\alpha)(1+n^{-1})$ in the previous inequality and using the definition of $\bar{\mathcal{C}}_\alpha(X_{n+1})$ given in (30) concludes the proof. □

B Experimental Setup and Results

B.1 Details of the experimental setup

We use the Mixture Density Network (Bishop, 1994) implementation from CDE (Rothfuss et al., 2019) Python package[2] as a base model for `CP`, `PCP` and `CP`[2]. The underlying neural network contains two hidden layers of 100 neurons each and was trained for 1000 epochs for each split of the data. Number of components of the Gaussian Mixture was set to 10 for all datasets.

For the `CQR` (Romano et al., 2019) and `CHR` (Sesia & Romano, 2021) we use the original authors' implementation[3]. The underlying neural network that outputs conditional quantiles consists of two hidden layers with 64 neurons each. Training was performed for 200 epochs for batch size 250.

For the `CPCG` (Gibbs et al., 2023) we also use the original authors' implementation[4]. We use the same splits and preprocessing steps as for other methods. The underlying prediction model is neural network with of two hidden layers of 64 neurons and is trained for 1000 epochs with early stopping. Embeddings from the last layer are collected to form feature maps, denoted as $\Phi(X)$ in the original paper. A linear functional class $\mathcal{F}$ is used. We fixed some minor bugs in the authors code to avoid an infinite loop and decreased maximum number of iterations to lower the computational cost.

For `LCP` (Guan, 2023) we once again used the original author's implementation[5]. The only change was that we supplied our own preprocessed and split data, the same for all the discussed methods. Most datasets had to be sub-sampled for training the model since the method computes full Hessian on the train set, its SVD decomposition and also uses cross-validation estimates of the residuals (scores). We kept all the hyperparameters values as in the original implementation.

We replicate the experiments for 50 random splits of all nine datasets. To lower noise in calculated performance metrics we reuse trained networks and samples across different top-level algorithms for each replication.

B.2 Worst-slab coverage

Here we present some additional experiments related to conditional coverage achieved by different methods. We have used Worst Slab Coverage metric, which is sensitive to the set of labs considered during the search. Following Cauchois et al. (2020); Romano et al. (2020b), recall that a slab is defined as

$$S_{v,a,b} = \left\{x \in \mathbb{R}^p : a < v^T x < b\right\},$$

where $v \in \mathbb{R}^p$ and $a, b \in \mathbb{R}$, such that $a < b$. Now, given the prediction set $\mathcal{C}_\alpha(x)$ and $\delta \in [0,1]$, the *worst-slab coverage* is defined as:

$$\mathrm{WSC}(\mathcal{C}_\alpha, \delta) = \inf_{v \in \mathbb{R}^p, a<b \in \mathbb{R}} \mathbb{P}\left(Y \in \mathcal{C}_\alpha(X) | X \in S_{v,a,b}\right) \; s.t. \; \mathbb{P}(X \in S_{v,a,b}) \geq 1-\delta.$$

In our experiments we follow Romano et al. (2020b) in our implementation of this metric. Namely, we use 25% of the data to find the worst slab and the use the remaining 75% to calculate the final value on this slab. We use 5000 randomly sampled directions, that are the same for each algorithm and change for each replication.

[2] https://github.com/freelunchtheorem/Conditional_Density_Estimation
[3] https://github.com/msesia/chr
[4] https://github.com/jjcherian/conditional-conformal
[5] https://github.com/LeyingGuan/LCP

B.3 EXTENDED RESULTS OF REAL DATA EXPERIMENTS

Table 2 we summarize all metrics from our real-world data experiments. For conditional coverage we report worst-slab coverage with $(1-\delta) = 0.1$. On six out of nine datasets CP^2 method achieves the best result in conditional coverage. In terms of interval width PCP method produces the narrowest intervals.As we can see, it happens at the expense of conditional coverage: PCP often achieves significantly lower values.

We also present a more detailed view of set size differences between the methods. In the main part we reported average rank of each method in Figure 8. We ranked the algorithms by their projected area at each test point and averaged the ranks. Here we show raw areas of the projections onto each pairs of axes for `sgemm_small` dataset in table 3. All targets were standardised to zero mean and unit standard deviation so that different projections will be in the same scale. We see that PCP produces smaller set sizes like in one-dimensional case. Quantile-regression based methods have the largest sets, even larger than the fixed-sized sets of CP. Our approach demonstrates only modest increase in prediction set size compared to PCP while achieving sharper conditional coverage.

Table 2: Summary results of experiments on real data. "M. Cov." stands for marginal coverage, "C. Cov." is the worst-slab coverage (here $(1-\delta) = 0.1$), and w_{sd} is average total length of the prediction sets, scaled by standard deviation of Y. Nominal coverage level is set to $(1-\alpha) = 0.9$. For $\Pi_{Y|X}$, PCP, CP^2−PCP we use the same underlying mixture density network model with 50 samples. CHR and CQR(2) also share the same base neural network model. We average results of 50 random data splits. For each dataset, we highlighted the algorithm achieving conditional coverage closest to the nominal level.

Dataset	Metric	CP	PCP	$\Pi_{Y\|X}$	CP^2 PCP-L	CP^2 PCP-D	CHR	CQR	CQR2
bike	M. Cov.	0.90	0.90	0.93	0.90	0.90	0.90	0.90	0.90
	C. Cov.	0.79	0.85	0.92	0.89	0.89	0.88	0.90	0.87
	w_{sd}	**0.71**	0.71	0.83	0.79	0.80	1.94	2.25	2.31
bio	M. Cov.	0.90	0.90	0.91	0.90	0.90	0.90	0.90	0.90
	C. Cov.	0.88	0.89	0.91	0.90	0.90	0.90	0.89	0.89
	w_{sd}	2.34	**1.89**	1.95	1.97	1.95	1.92	2.13	2.10
blog	M. Cov.	0.90	0.90	0.91	0.90	0.90	0.90	0.90	0.90
	C. Cov.	0.60	0.74	0.91	0.89	0.90	0.87	0.87	0.86
	w_{sd}	0.60	**0.30**	0.72	0.72	0.71	0.31	0.44	0.39
fb1	M. Cov.	0.90	0.90	0.93	0.90	0.90	0.90	0.90	0.90
	C. Cov.	0.49	0.64	0.92	0.88	0.89	0.87	0.90	0.87
	w_{sd}	0.47	0.28	0.58	0.56	0.59	**0.26**	0.37	0.33
fb2	M. Cov.	0.90	0.90	0.93	0.90	0.90	0.90	0.90	0.90
	C. Cov.	0.50	0.61	0.91	0.88	0.88	0.88	0.89	0.89
	w_{sd}	0.53	**0.32**	0.65	0.62	0.65	0.33	0.43	0.37
meps19	M. Cov.	0.90	0.90	0.89	0.90	0.90	0.90	0.89	0.90
	C. Cov.	0.54	0.78	0.89	0.90	0.89	0.90	0.88	0.89
	w_{sd}	1.05	**0.73**	1.02	1.19	1.07	0.76	1.14	1.19
meps20	M. Cov.	0.90	0.90	0.89	0.90	0.90	0.90	0.90	0.90
	C. Cov.	0.58	0.80	0.89	0.90	0.90	0.91	0.88	0.89
	w_{sd}	1.06	**0.75**	0.98	1.15	1.04	0.77	1.09	1.17
meps21	M. Cov.	0.90	0.90	0.89	0.90	0.90	0.90	0.90	0.90
	C. Cov.	0.54	0.81	0.89	0.89	0.89	0.90	0.89	0.88
	w_{sd}	1.04	**0.72**	0.99	1.16	1.04	0.79	1.13	1.21
temp	M. Cov.	0.90	0.90	0.82	0.90	0.90	0.90	0.90	0.90
	C. Cov.	0.87	0.89	0.81	0.88	0.89	0.86	0.85	0.86
	w_{sd}	0.87	0.92	**0.78**	0.96	0.93	1.31	1.48	1.30

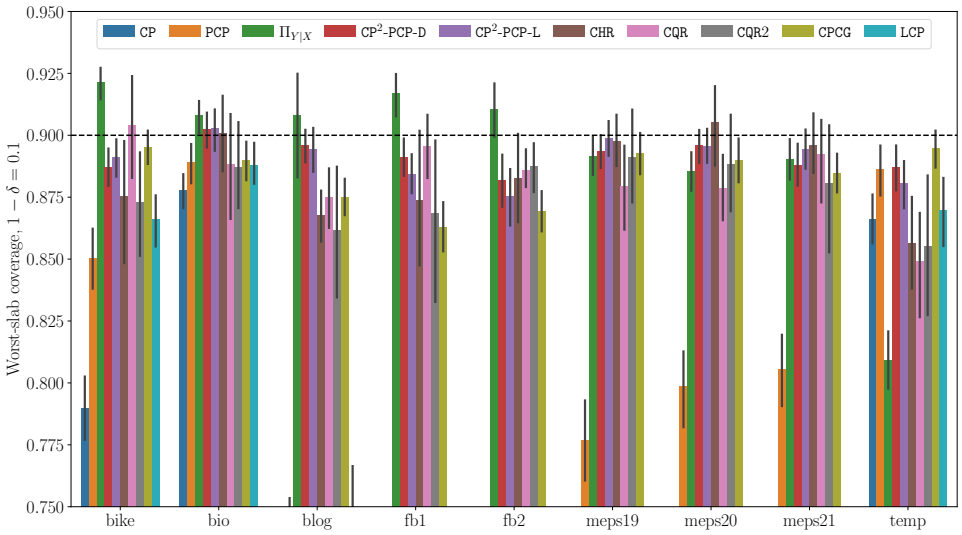

Figure 9: Worst-slab coverage on real data (mean and stdev.). Results averaged over 50 random splits of each dataset. Calibration and test set sizes set to 2000, 50 conditional samples for PCP, CP^2 and $\Pi_{Y|X}$. Worst-slab coverage parameter $(1-\delta)=0.1$. Nominal coverage level is $(1-\alpha)=0.9$ and is shown in dashed black. Methods with conditional coverage below 0.75 are not shown.

Table 3: Prediction set size comparison for sgemm_small dataset. Rows correspond to different pairs of targets (dataset has 4 targets). For each method the reported value is the mean area of the 2D projection of the prediction set to the corresponding axes pair.

				CP^2				
Axes	CP	PCP	$\Pi_{Y\|X}$	PCP-L	PCP-D	CHR	CQR	CQR2
(0, 1)	2.137	0.435	0.517	0.576	0.560	2.290	2.550	2.436
(0, 2)	2.145	0.435	0.518	0.577	0.561	2.267	2.506	2.358
(0, 3)	2.145	0.436	0.519	0.578	0.561	2.086	2.366	2.172
(1, 2)	2.146	0.435	0.517	0.576	0.560	2.388	2.622	2.546
(1, 3)	2.146	0.435	0.517	0.576	0.560	2.166	2.461	2.314
(2, 3)	2.154	0.436	0.519	0.578	0.562	2.153	2.430	2.255

B.4 Other perspective on conditional coverage

The worst-slab coverage metric used in the previous section is not always helpful: (1) it provides a single number for each method, and (2) the selected slab is different for each algorithm. In practice we might be interested in how sharp the coverage is along the portion of the input space spanned by the test data. To explore this, we used two approaches: dimensionality reduction and clustering. Results for clustering with HDBSCAN are presented in the main part in Figure 5, here turn to dimensionality reduction.

First we apply UMAP algorithm to project data to two dimensions and then construct a heatmap plot to show coverage in each bin of the histogram. Results for meps_19 dataset are presented in Figure 10. Nominal coverage is set to $(1-\alpha)=0.9$ and corresponds to gray part of the color scale. We can see that our method and baseline $\Pi_{Y|X}$ perform better than CP and PCP across the space.

B.5 Additional synthetic data experiments

To extend our toy one-dimensional example from the main part, we also test out our algorithm and other methods on a synthetic dataset with multiple input dimensions. We use the heteroscedastic sampling procedure from Shukla et al. (2024) [6] to generate a dataset with 10000 instances, 10

[6] https://github.com/vita-epfl/TIC-TAC/tree/main

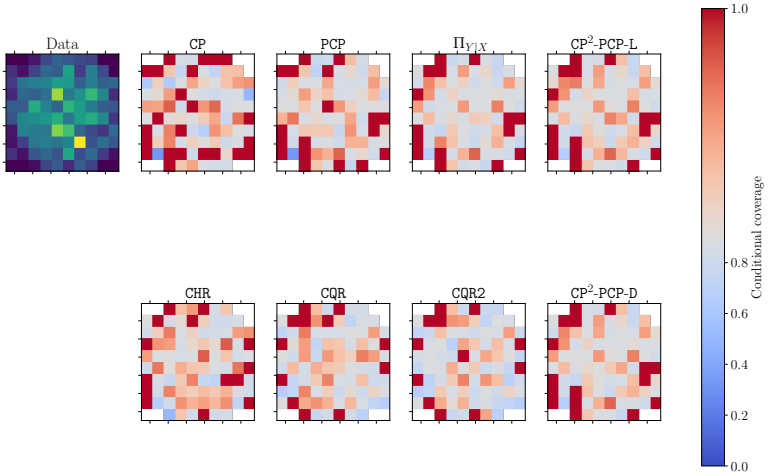

Figure 10: Conditional coverage after dimensionality reduction, `meps_21` dataset. Data projected to two dimensions using UMAP algorithm with Canberra metric, with the `n_neighbors` hyperparameter set to 2. Nominal coverage is set to $(1 - \alpha) = 0.1$, it corresponds to gray on the color scale.

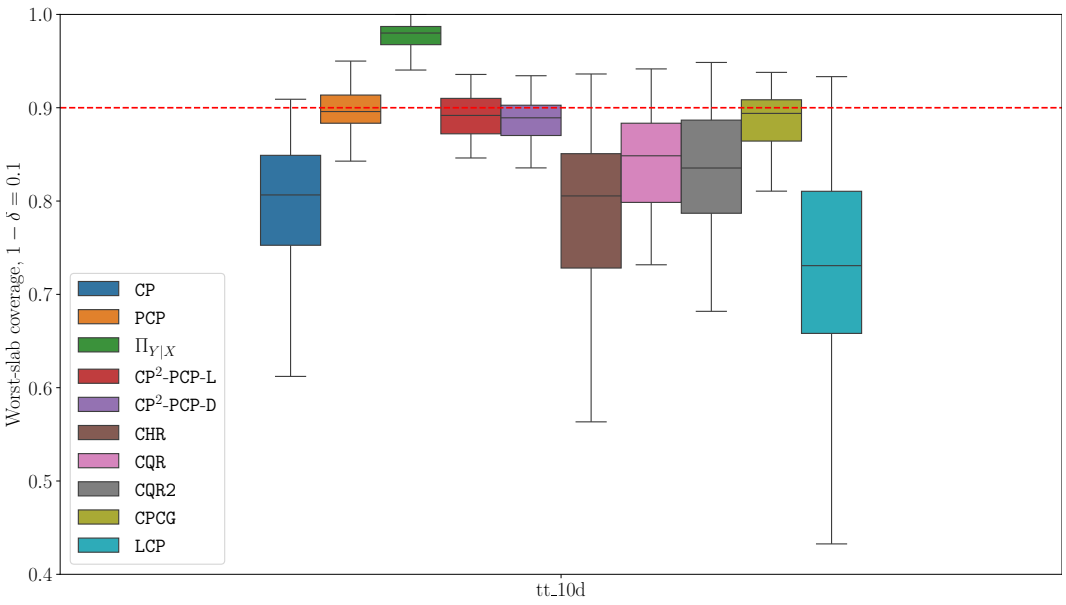

Figure 11: Conditional coverage for synthetic data. Nominal coverage is set to $(1 - \alpha) = 0.1$, shown in dashed red.

input features and one output that we name `tt_10d`. True distribution $P_{Y|X}$ is Gaussian but has variable variance. We follow the same evaluation protocol as for our main experiments and results are summarized in figures 11, 12.

On this data most methods provide adequate results with the exception on `LCP`, which significantly undercovers and produces wide intervals. In terms of conditional coverage our method, `PCP` and `CPCG` show very sharp conditional coverage. In terms of prediction set size our method is very close to competition albeit a bit higher. Considering the ability of `CP`^{2}`-PCP` to handle multi-modal targets we see it as a good result.

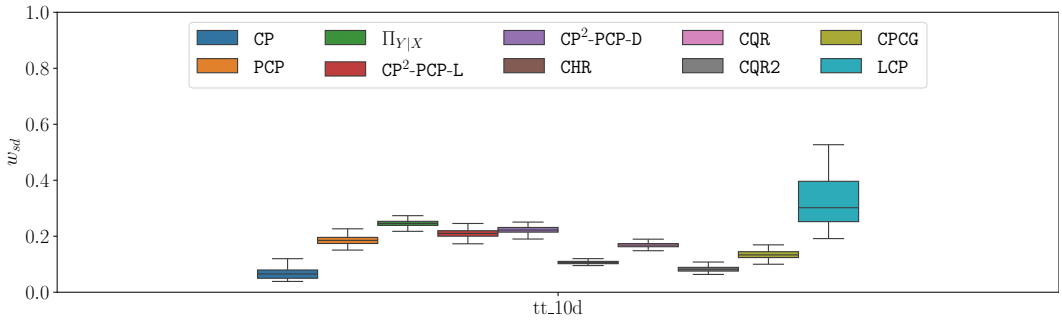

Figure 12: Sizes of the prediction sets on synthetic data. We divide the size of the set by the standard deviation of response to present the results on the same scale.

C Additional discussions

C.1 Highest predictive density (HPD) regions

CP^2 with Explicit Conditional Density estimate: CP^2-HPD. Assume that an estimator the conditional density function is known, denoted by $\gamma_{Y|X=x}$. The confidence set is defined as $\mathcal{R}(x;t) = \{y \in \mathcal{Y}\colon \gamma_{Y|X=x}(y) \geq -t\}$. We omit the variable z from the notation, as we do not consider exogenous randomization in this case. The parameter τ_x is obtained by solving

$$\tau_x = \arg\min \left\{ \tau \in \mathbb{R}\colon \int_{\mathcal{R}(x;\tau)} \gamma_{Y|X=x}(y)\,\mathrm{d}y \geq 1-\alpha \right\}. \tag{31}$$

We then compute $\lambda_{x,y} = -\gamma_{Y|X=x}(y)$ and derive the prediction set as

$$\mathcal{C}_\alpha(x) = \left\{ y \in \mathcal{Y}\colon \gamma_{Y|X=x}(y) \geq -f_{\tau_x}\left(Q_{1-\alpha}\left(\mu_n\right)\right) \right\}.$$

If we take $f_\tau(\lambda) = \lambda$ and $\varphi = 1$, the method shares similarity with the `CD-split` method, proposed in Izbicki et al. (2020). While `CD-split` uses $\lambda_{x,y}$ as the conformity score, our method uses $f_{\tau_x}^{-1}(\lambda_{x,y})$, which incorporates the information from τ_x to modify $\gamma_{Y|X=x}(y)$. The `CP`^{2}`-HPD` workflow is summarized in Algorithm 2.

Of course, the computation of (31) is in general highly non-trivial. Izbicki et al. (2020) suggested to use binning, therefore approximating the conditional predictive distribution with histograms. The method is restricted to the case where the dimension of $\mathcal{Y}$ the response is small; see Izbicki et al. (2020) for the case of $\mathcal{Y} = \mathbb{R}$. When the dimension becomes larger, then the estimation of HPD is typically based on Monte Carlo methods, thus requiring the introduction of auxiliary variables.

The HPD set is theoretically the optimal confidence region in terms of size. Izbicki et al. (2022) developed two algorithms, CD-split and HPD-split, which converge to the HPD set; see Theorem 27 and Theorem 28. In HPD-split, the conformity score is $\widehat{H}(\widehat{f}(y|x)|x)$ rather than $\widehat{f}(y|x)$, where $H(z|x)$ approximates the conditional CDF of $f(Y|X)$. This ensures that $H(f(Y|X)|X) \sim U(0,1)$ given X, which implies that $H(f(Y|X)|X)$ is independent of X. Consequently, if $\widehat{f}(y|x)$ converges to $f(y|x)$, it is expected that $\widehat{H}(\widehat{f}(Y|X))$ becomes approximately independent of X. However, computing $H(f(Y|X)|X)$ requires integrating the conditional density, which can be challenging in high-dimensional spaces.

Our `CP`^{2}`-PCP` method offers a more practical approach for high-dimensional settings by generating balls centered at sampled points with radii set in function of x. This adaptive radius helps mitigate the issues of under-coverage or over-coverage often encountered with PCP. Additionally, the prediction set being a union of balls, is particularly beneficial when dealing with multimodal data.

NAME	$f_\tau(\lambda)$	$f_\tau^{-1}(\lambda)$	φ
Linear	$\tau\lambda$	$\tau^{-1}\lambda$	1
Difference	$\tau+\lambda$	$\lambda-\tau$	0

Table 4: Adjustment Functions f_t, their inverses f_τ^{-1} and φ values used in our experiments.

Algorithm 2 CP^2-HPD

Input: dataset $\{(X_k, Y_k)\}_{k\in[n]}$, significance α, conditional density $\gamma_{Y|X}$, function f_t.
// Compute the $(1-\alpha)$-quantile
for $k = 1$ **to** n **do**
  Set $\bar{\lambda}_k = -\gamma_{Y|X=X_k}(Y_k)$
  Set $\bar{\tau}_k = \tau_{X_k}$ as given in (3)
$Q_{1-\alpha}(\mu_n) \leftarrow \lceil (1-\alpha)(n+1)\rceil$-th smallest value in $\{f^{-1}_{\bar{\tau}_k}(\bar{\lambda}_k)\}_{k\in[n]} \cup \{\infty\}$
// Compute the prediction set for a new point $x \in \mathbb{R}^d$
Compute τ_x in (3).
Output: $\mathcal{C}_\alpha(x) = \{y \in \mathcal{Y} \colon \gamma_{Y|X=x}(y) \geq -f_{\tau_x}(Q_{1-\alpha}(\mu_n))\}$.

C.2 DISCUSSION ON THE ASSUMPTIONS

H1: Assumption on the shape of confidence regions. This assumption does not impose restrictive constraints on the shape of the confidence regions. It allows for a broad class of geometries, making it widely applicable. Most prediction sets proposed in the literature naturally satisfy this assumption. For instance, it permits level sets of a density function or unions of ellipsoidal regions.

H2: Monotonicity of $\tau \mapsto f_\tau(\varphi)$. We assume that the function $\tau \mapsto f_\tau(\varphi)$ is monotonic and specifically increasing. This property ensures that the region $R(x; f_{\tau_x}(\varphi))$ expands as the parameter τ_x increases. This assumption is crucial because we want the confidence region to grow in size as the parameter τ_x increases.

H3: Convergence in total variation. This assumption ensures the convergence of $P_X \otimes \Pi_{Y|X}$ to $P_X \otimes P_{Y|X}$ in total variation. While this condition is essential for the theoretical validity of our approach, it is also the most challenging to verify in practice. Kernel-based density estimators satisfy this condition under specific choices of the kernel function and the bandwidth parameter; see for example Devroye & Lugosi (2001, Chapter 9) and Li et al. (2022).

C.3 DISCUSSION ON f_t

We present examples of mappings f_t and their inverses f_τ^{-1} in Table 4. The choice of the mapping f_t is crucial for the performance of the method, and we investigate their impact in Section 4. For instance, choosing $f_\tau(\lambda) = \tau\lambda$ results in approximately conditionally valid prediction sets, as long as $\Pi_{Y|X=x}$ accurately estimates the conditional distribution $\mathrm{P}_{Y|X=x}$; see Theorem 3.2-Theorem 3.3. Initially we also considered other adjustment functions based on exponent, sigmoid and $\tanh$ functions, but they all performed worse than linear and sum. As we show in 2, these two selected adjustment function perform similarly, showing only marginal differences on some datasets. Designing new adjustment functions is a possible future research direction.